AD-A273 807

PARAMETRIC AND NONPARAMETRIC DISCRIMINANTS FOR REGIONAL EARTHQUAKES AND EXPLOSIONS

Joseph E. Cavanaugh
Allan D.R. McQuarrie
Robert H. Shumway

University of California
Division of Statistics
Davis, CA 95616

DTIC
S ELECTE
NOV 02 1993
E D

31 July 1993

Scientific Report No. 2

Approved for public release; distribution unlimited

93-26427

PHILLIPS LABORATORY
Directorate of Geophysics
AIR FORCE MATERIEL COMMAND
HANSCOM AFB, MA 01731-3010

93 11 1 015

The views and conclusions contained in this document are those of the authors and should not be interpreted as representing the official policies, either expressed or implied, of the Air Force or the U.S. Government.

This technical report has been reviewed and is approved for publication.

JAMES F. LEWKOWICZ
Contract Manager
Solid Earth Geophysics Branch
Earth Sciences Division

JAMES F. LEWKOWICZ
Branch Chief
Solid Earth Geophysics Branch
Earth Sciences Division

DONALD H. ECKHARDT, Director
Earth Sciences Division

REPORT DOCUMENTATION PAGE

Public reporting burden for this collection of information is estimated to average 1 hour per response, including the time for reviewing instructions, searching existing data sources, gathering and maintaining the data needed, and completing and reviewing the collection of information. Send comments regarding this burden estimate or any other aspect of this collection of information, including suggestions for reducing this burden, to Washington Headquarters Services, Directorate for Information Operations and Reports, 1215 Jefferson Davis Highway, Suite 1204, Arlington, VA 22202-4302, and to the Office of Management and Budget, Paperwork Reduction Project (0704-0188), Washington, DC 20503.

1. AGENCY USE ONLY (Leave blank)	2. REPORT DATE	3. REPORT TYPE AND DATES COVERED
	July 31, 1993	Scientific No. 2

4. TITLE AND SUBTITLE	5. FUNDING NUMBERS
Parametric and Nonparametric Discriminants for Regional Earthquakes and Explosions	Contract F19628-91-K-0033 PE69120C PRT121 TATC WUAB

6. AUTHOR(S)

Joseph E. Cavanaugh
Allan D.R. McQuarrie
Robert H. Shumway

7. PERFORMING ORGANIZATION NAME(S) AND ADDRESS(ES)	8. PERFORMING ORGANIZATION REPORT NUMBER
Division of Statistics University of California Davis, CA 95616	Division of Statistics Technical Report #290

9. SPONSORING/MONITORING AGENCY NAME(S) AND ADDRESS(ES)	10. SPONSORING/MONITORING AGENCY REPORT NUMBER
Phillips Laboratory 29 Randolph Road Hanscom AFB, MA 01731-3010 Contact Manager: J. Lewkowicz/GPEH	PL-TR-93-2164

11. SUPPLEMENTARY NOTES

12a. DISTRIBUTION/AVAILABILITY STATEMENT	12b. DISTRIBUTION CODE
Approved for Public Release; Distribution Unlimited	

13. ABSTRACT (Maximum 200 words)

Conventional methods for discriminating between earthquakes and explosions at regional distances have concentrated on extracting specific features such as amplitude and spectral ratios from the waveforms of the P and S phases. We consider here an optimum nonparametric classification procedure derived from the classical approach to discriminating between two Gaussian processes with unequal spectra. Two robust variations based on the minimum discrimination information statistic and Renyi's entropy are also considered. We compare the optimum classification procedure with various amplitude and spectral ratio discriminants and show that its performance is superior when applied to a small population of 8 land-based earthquakes and 8 mining explosions recorded in Scandinavia. Several parametric characterizations of the notion of complexity based on modeling earthquakes and explosions as autoregressive or modulated autoregressive processes are also proposed and their performance compared with the nonparametric and feature extraction approaches.

14. SUBJECT TERMS			15. NUMBER OF PAGES
Discrimination, Scandinavian events, Spectral features, Quadratic detection, Information theory.			54
			16. PRICE CODE

17. SECURITY CLASSIFICATION OF REPORT	18. SECURITY CLASSIFICATION OF THIS PAGE	19. SECURITY CLASSIFICATION OF ABSTRACT	20. LIMITATION OF ABSTRACT
Unclassified	Unclassified	Unclassified	SAR

TABLE OF CONTENTS

Accesion For		
NTIS CRA&I		☒
DTIC TAB		☐
Unannounced		☐
Justification		
By		
Distribution /		
Availability Codes		
Dist	Avail and/or Special	
A-1		

1. Introduction

Conventional methods for discriminating between earthquakes and explosions at regional distance have concentrated on extracting *specific features* from the waveforms of the P(usually P_g) and S (usually L_g) phases. The specific features considered generally are amplitude ratios, measures of waveform complexity or various kinds of spectral ratios, suggesting that the main characterization of the differences between earthquakes and explosions reduces to differences between the spectra or differences between the waveforms. Our objective here is to compare some of the classical discriminants in the literature with two methods based on *statistical optimality criteria*. We consider first an *optimal nonparametric discriminator*, derived under the assumption that the earthquake and explosion P and S phases are uncorrelated stationary Gaussian processes with unequal spectra. The likelihood criterion that obtains displays the optimal statistic as the result of comparing spectral matches between the observed series and the average earthquake spectrum against a comparable match with the explosion spectrum. Two variations based on information theoretic principles are also investigated. A *parametric discriminator* models the P phase as a modulated autoregressive process, where the modulating function is consistent with models for earthquake and explosion waveforms found in the literature. The nonparametric method is obviously tuned to spectral differences whereas the parametric method is closely allied with notions relating to complexity and amplitude ratios.

Numerous investigators have pointed out that the logarithms of P_g/L_g amplitude ratios tend to be lower for earthquakes than for explosions (see, for example Blandford, 1981, Bennett and Murphy, 1986, Taylor et al, 1989). This idea has been extended to include a consideration of spectral ratios involving the P and S groups. Bennett and Murphy (1986) note that for western U.S. events, earthquake L_g spectra contained more high frequencies, and that the ratio of the logarithms of low frequency (.5-1 Hz) L_g to higher frequency L_g (2-4 Hz) tend to be larger for explosions. Taylor et al (1989) also use this ratio over the frequency bands (1-2 Hz) and (6-8 Hz) and extended the consideration to the P_g phase. Dysart and Pulli (1990, 1992) have also considered various spectral ratios P/S for Scandinavian events and have developed neural networks as an alternative to simple linear combinations of features for discrimination. They note that the P/S spectral ratios are generally higher for explosions than for earthquakes. Finally, Kim et al (1992) note that for eastern U.S. events the ratios of P_g to L_g spectra are generally higher for explosions. Some early results using the three coefficients in an third-order autoregressive model for the coda as features are available in Tjøstheim (1974).

1

The spectral methods discussed above generate *features* that can differ for earthquakes and explosions in certain specific data bases. Such features as P to S amplitude ratios or spectral ratios within phases or between phases can then be put into a vector and transformed (usually, logarithms are taken for a better approximation to normality) in order to apply one of the standard linear or quadratic discriminant analysis techniques. Examples are Shumway and Blandford (1974), Taylor et al (1989), Dysart and Pulli (1990), Pulli and Dysart (1992) and Kim et al (1992). Two features at a time are often plotted in various combinations for earthquakes and explosions to show graphically the separation of the two populations (see the above references and also Bennett and Murphy, 1986).

Shumway and Blandford (1974) introduced an optimal method combining optimal linear and quadratic discriminant functions. The criterion was based on modeling the underlying short period teleseismic P waveforms as Gaussian processes differing in both the mean value signals and the spectral densities. For regional events, it is clear that the notion of a fixed mean P or S waveform which differs for earthquakes and explosions is not a relevant comparison but that the notion that the earthquakes and explosions differ only in their spectra does make a lot of sense. This implies that the quadratic part of the optimal detector used by Shumway and Blandford (1974) (see also Shumway, 1982, 1988) will have the lowest misclassification rate of *any function* based on the spectra, including those given in the preceding paragraph. Such a detector has been applied several times in the literature to seismic discrimination, by other investigators as well (see, for example Dargahi-Noubary and Laycock, 1981, Alagon, 1989). We develop and apply a modified version of such a detector to P and S phases from population of regional Scandinavian earthquakes and explosions given in Blandford (1993). Since the model depends only on stationarity of the series and not on a specific parametric model for the spectrum, we refer to it as the *optimal nonparametric discriminator.*

Modifications to the nonparametric version of the likelihood detector can be made based on information theoretic principles. For example, the optimum quadratic detector has an information theoretic interpretation in terms of the *minimum discrimination information statistic* (MDI), of Kullback (1978). Such a discriminant, defined as the difference of the discrepancies between the sample spectrum of the event to be classified and the theoretical earthquake and explosion spectra, has excellent theoretical properties as discussed by Zhang and Taniguchi (1992, 1993). They suggest an alternate discriminant that is robust to peak contamination which is based on the Renyi index of index α as discussed by Parzen (1990) (see Renyi, 1961). Zhan and Taniguchi call the discriminant the *α-entropy.* We will apply the MDI and Zhang-Taniguchi (ZT) discriminants to the earthquake and

explosion populations and show that the ZT discriminant offers several advantages over the conventional likelihood discriminant.

Blandford (1993) discusses a notion of complexity as a discriminant and shows that it has potential for discrimination of the events in the Scandinavian database. The idea relates to the often quoted statement by analysts that complexity is a strong component of their visual procedure for discrimination. Blandford proposes a notion of complexity related to the observation that explosions generate usually an *impulsive signal* whereas earthquakes tend to generate a more *emergent signal*. We develop here a *parametric discriminator* by assuming that the earthquake and explosion populations can be expressed as uniformly modulated autoregressive process; parameters of the modulating function characterize separately the emergent and impulsive properties of the signal. Our underlying model for complexity is taken directly from a suggestion of Dargahi-Noubary (1992) that is based on standard source theory.

2. Data Compilation

For our test data, we use a subset of stations recording 8 earthquakes and 8 explosions in Scandinavia from the arrays NORESS, ARCESS and FINESS as described in Blandford (1993). According to Blandford, "The events were selected with consideration for having sufficient S/N at single elements so that all phases could be clearly seen on all components of a single instrument $\cdots$". From Table 1 in Blandford, we took explosions three through ten and from Table 2, we used all eight earthquakes. All events chosen by Blandford were on or near land and were distributed uniformly over Scandinavia to minimize the possibility that discriminators might be keying on location or land-sea differences. Figure 1 shows portions of typical earthquakes and explosions (sampled at 20 Hz) along with the portions of the record that we visually determined as the P and S phases. We did not identify specific phases through velocity computations but simply chose fairly broad (25 second) windows that seemed to include the P and S phases.

Qualitatively, we note that the earthquake has a much smaller amplitude P/S ratio than the explosion and we note the relatively complex P phase which tends to be emergent for the earthquake as compared with the generally impulsive P phase signals from the explosions. These comparisons, if universal, would make discrimination quite easy but a casual inspection of Figures A1-A16 in the Appendix shows that this is not universally true. For example Earthquakes 4 and 5 in Figures A4 and A5 have relatively large P/S amplitude ratios, more like that of an explosion although they still display the emergent

3

P phases. For explosions in Figures A9-A16 the P/S amplitudes are generally higher than for earthquakes although Explosion 1 in Figure A1 is an exception. Explosions 4 and 5 have slightly more emergent P phases although the distinctly high single peak in Explosion 5 indicates that the event may be an explosion. The earthquakes in Figures A1-A8 do not display such sharp initial pulses.

The autoregressive (based on a third order AR model) spectra were computed for the P and S phases for all earthquakes and explosions. This assumption is not inconsistent with source models assuming a decay inversely proportional to ν^3 where ν is frequency. Fitting a low order AR spectrum also tends to de- emphasize spurious peaks and values due to ripple firing of the mine explosions. The AR spectra shown in Figures A1-A8 for earthquakes tend to have stronger low frequencies in the S phases (0-5 Hz) and higher frequency content in the P phases (5-8 Hz) for earthquakes. Explosions generally tend to have peaks at roughly the same frequency which varies over the 5-8 Hz range. Explosions 1 and 8 in Figure A9 and A16 have low to high frequency behavior consistent with that just mentioned for earthquakes so the spectral discriminant is not absolutely reliable either.

To make overall qualitative assessments it is easiest to look at the average spectra of the earthquake and explosion groups separately. Figure 2 shows these average spectra where all traces have been scaled by dividing by the maximum amplitude of the P phase. We have plotted on a linear scale since this emphasizes spectral differences in the high signal to noise parts of the earthquake and explosion processes. The top left panel shows the average spectra plotted on different scales indicated on the left and right ordinates. This display scales out amplitude differences and allow us to see the spectral shape contrasts. For the P phases, we notice a broader spectrum with both high and low frequencies; the main differences appear to be in the low (0-6 Hz) band. We note that in the top right panel, which plots the spectra on the same scale, the differences seem to be characterized by a stronger low frequency (0-6 Hz) component for earthquake P than one sees in the high frequency (6-15 Hz) band. The S components shown in the bottom panels are more narrow band and relatively higher for earthquakes in the interval (0-3 Hz) and higher for explosions in the (3-12 Hz) band.

It seems clear that the process of guessing spectral ratios by looking at separate or average spectra will lead to a number of possible discriminants as can be seen by examining the literature. In the next section, we consider some amplitude and spectral discriminants that have been proposed in the seismic literature and show that features extracted from the amplitude characteristics do best for the small sample of earthquakes and explosions given above.

4

3. Discriminants Based on Amplitude and Spectral Features

For feature extraction, we consider a number of classical measures related to the spectrum. They are logarithms of (1) P and S amplitudes, (2) P and S mean square error, (3) combinations of P and S spectra (0-3 Hz, 3-6 Hz, 6-9 Hz) and (4) autoregressive coefficients of the P and S phases for a third order model. The frequency ranges were not exactly comparable to those used in the literature (.5-1Hz, 2-4 Hz in Bennett and Murphy, 1986, 1-2 Hz, 6-8 Hz in Taylor et al, 1989, 2-5 Hz, 5-10 Hz, 10-20 Hz in Pulli and Dysart, 1993, 5-25(5) Hz in Kim et al, 1992) but were chosen by visually inspecting the separate spectra and the average earthquake and explosion spectra shown in Figure 2. A further comment is that we have avoided taking ratios of spectra which tend to assume a-priori that the best discriminator will be the simple difference of the form $\log(P/S) = \log P - \log S$. It is clear from our results that the log ratio is nearly the best discriminant and it is also reasonable that taking logarithms improves the approximations to multivariate normality.

The best discriminators of this group were the classical amplitude and mean square error measures (1) and (2); (1) is plotted in Figure 3 and the scatter diagram of the mean square error (2) hardly differs from this top panel. A linear discriminant analysis with equal prior probabilities tended to confirm the ratio procedure. For example the optimal linear discriminant functions for P and S amplitudes and mean square errors were

$$d_{(1)} = -20.59 \log P + 15.97 \log S + 14.32$$

and

$$d_{(2)} = -15.02 \log P + 13.30 \log S - 25.40$$

respectively. Both (1) and (2) had perfect classification in the test sample and classified the first explosion as an earthquake in the holdout-one procedure.

Note that the hold-out procedure (see Lachenbruch and Mickey, 1968) gives reasonable approximations for the misclassification rates that would obtain when classifying a new observation not in the training sample. The holdout procedure estimates the discriminant function for each observation with that observation held out of the training sample. The linear discriminant function obtained is then applied to the observation that was held out. The misclassification rates for all methods using the original sample and the hold-out procedure are shown in Table 1.

The best of the spectral group (3), also plotted in Figure 3, focusses on the (0-3 Hz) frequency band where differences were noted in Figure 2. Of course, this is bound to be

closely related to P/S amplitude (1) and the mean square error (2) which are both closely related to the low frequency power. It is not surprising that it has the same performance as (1) and (2), leading to a linear discriminant function of the form

$$d_{(3)} = -13.07 \log P + 12.99 \log S - 10.94.$$

Note that all discriminant functions are essentially of the form $-\log P/S$. This confirms the intuitive use of measures of the form $\log P/S$ which is common in the seismology literature. The other techniques in (3) (see Figures 4 and 5) gave inferior performances and Method (4), suggested by Tjøstheim (1975) had the worst performance with almost no discrimination capability. This is surprising because the third-order AR spectra in Figures A1-A16 seem to do a reasonable job of characterizing the spectra and because one might expect from standard source theory arguments that such a process would fit the data. In general, the third-order AR predictions miss the impulsive excursions of the explosions. We have not investigated combining more than two spectral discriminants because of the small training samples (8 earthquakes and 8 explosions) involved in the comparisons. Global frequency discriminants have been considered in the literature for larger samples by Pulli and Dysart (1992), Taylor et al (1989) and Kim et al (1992). Such global discriminants (see, for example, Kim et al, 1992) can often lead to linear combinations with both positive and negative coefficients. One is hard put to develop an intuitive rationale for using such combinations.

A comparison of performances on the small test sample of Scandinavian events is given in Table 1. We include the measures based on likelihood and information theoretic arguments given Section 4 and the complexity approach given in Section 5. We note the slight overall superiority of the global optimality measures and the general satisfactory performance of the P/S amplitude based discriminants considered in the literature. The specific spectral ratios do less well although it is clear that the optimal tuning to the spectra represented by the likelihood and information theoretic methods can do very well indeed.

Table 1: Misclassifications (* = Holdout)

Method	EQ	EXP	EQ*	EXP*
Amplitude				
$\log_{10} P, \log_{10} S$	0	0	0	1
Spectral Discriminants				
MSE ($\log_{10} P, \log_{10} S$)	0	0	0	1
$\log_{10} P(0\text{-}3), \log_{10} S(0\text{-}3)$	0	0	0	1
$\log_{10} P(6\text{-}9), \log_{10} S(6\text{-}9)$	1	2	2	3
$\log_{10} S(0\text{-}3), \log_{10} S(3\text{-}6)$	1	4	0	4
Optimal Quadratic	0	0	0	0
MDI	0	0	0	0
ZT	0	0	0	0
Complexity				
θ_1, θ_2	2	2	2	2

4. Optimal Spectral Discriminants

For our *optimal nonparametric* classification procedure, consider the classical approach to discriminating between two stationary bivariate Gaussian processes (H_1 : Earthquakes and H_2 : Explosions) with unequal matrix covariance functions (spectra). An approximation (see, for example, Shumway, 1988) to the optimal test statistic is related to the match between the Fourier spectrum of the series of unknown origin and the spectrum of the earthquake or explosion process. Consider the likelihood or matching function under $H_j, j = 1, 2$, given by

$$ d_{j\cdot} = -\frac{1}{2} \sum_{k=0}^{T-1} \left\{ \log f_{j\cdot}(\nu_k) + \frac{|X_{\cdot}(k)|^2}{f_{j\cdot}(\nu_k)} \right\}, \tag{1} $$

where we replace · by P or S depending on the phase to be considered, $X_{\cdot}(k)$ is the discrete Fourier transform of the data $x_{t\cdot}$ and $f_{j\cdot}(\nu_k)$ denotes the spectrum for phase · under hypothesis H_j. The frequencies are of the form $\nu_k = k/T, k = 0, \ldots, T - 1$. The optimal statistic for testing whether the sampled bivariate series is from $H_1 : EQ$ or from $H_2 : EXP$ is given by

$$ Q = (d_{1P} - d_{2P}) + (d_{1S} - d_{2S}), \tag{2} $$

7

where we accept H_1 (earthquake) if $Q > 0$ and H_2 (explosion) if $Q \leq 0$. Note that the P and S phases need to be uncorrelated processes for this detector to be optimal. We have computed cross spectra and coherence functions of the paired phases for every event and they are not significantly greater than zero.

We may also look at information theoretic approaches to discriminating between two processes. It is known (see Shumway and Unger, 1974) that the *discrimination information* for two Gaussian processes differing only in the spectra is approximately

$$I(f_{1\cdot}, f_{2\cdot}) = \frac{1}{2} \sum_{k=0}^{T-1} \left\{ \frac{f_{1\cdot}(\nu_k)}{f_{2\cdot}(\nu_k)} - \log \frac{f_{1\cdot}(\nu_k)}{f_{2\cdot}(\nu_k)} - 1 \right\}. \tag{3}$$

Generally, it is convenient to regard the quantity given above as a measure of the *discrepancy* between the two spectral densities $f_{1\cdot}(\nu_k)$ and $f_{2\cdot}(\nu_k)$ since $I(f_{1\cdot}, f_{2\cdot}) \geq 0$ with equality if and only if $f_{1\cdot}(\nu_k) = f_{2\cdot}(\nu_k)$ for all k. Kullback (1978) has developed the *minimum discrimination information* (MDI) criterion as a means for classifying a new observation into H_1 or H_2. Under this principle, one compares the discrepancy of a spectral estimator computed from the sample realization $x_{t\cdot}$, say $f_{T\cdot}(\nu_k)$ with $f_{1\cdot}(\nu_k)$ and $f_{2\cdot}(\nu_k)$ using

$$I(f_{1\cdot}, f_{2\cdot}; f_{T\cdot}) = I(f_{T\cdot}, f_{2\cdot}) - I(f_{T\cdot}, f_{1\cdot}), \tag{4}$$

where

$$I(f_{T\cdot}, f_{j\cdot}) = \frac{1}{2} \sum_{k=0}^{T-1} \left\{ \frac{f_{T\cdot}(\nu_k)}{f_{j\cdot}(\nu_k)} - \log \frac{f_{T\cdot}(\nu_k)}{f_{j\cdot}(\nu_k)} - 1 \right\}. \tag{5}$$

Since we want the discrepancy between the sample spectrum and the true density to be minimized, it is clear that we should accept H_1 when $I(f_{1\cdot}, f_{2\cdot}; f_{T\cdot}) \geq 0$ and accept H_2 otherwise. In terms of the overall criterion, expressed in terms of both phases we would choose H_1 (earthquake) when

$$I(f_{1\cdot}, f_{2\cdot}; f_{TP}) + I(f_{1\cdot}, f_{2\cdot}; f_{TS}) \geq 0. \tag{6}$$

Note that for $f_{T\cdot}(\nu_k) = |X_{\cdot}(k)|^2$, the periodogram estimator, the above criterion reduces exactly to the quadratic criterion defined in Equation (1). Zhang and Taniguchi (1992) have shown the asymptotic normality of the MDI criterion and that the misclassification

8

errors converge to zero. They have also shown that the criterion is robust to departures from normality.

Zhang and Taniguchi (1993) have also suggested the α-*entropy*

$$e_\alpha(f_{1\cdot}, f_{2\cdot}) = \frac{1}{2} \sum_{k=0}^{T-1} \left\{ \log\left(1 - \alpha + \alpha \frac{f_{1\cdot}(\nu_k)}{f_{2\cdot}(\nu_k)} \right) - \alpha \log \frac{f_{1\cdot}(\nu_k)}{f_{2\cdot}(\nu_k)} \right\} \tag{7}$$

$0 < \alpha, 1)$ as an alternative and show that it is robust to both non-Gaussian departures and peak contamination. Under this suggestion, we would accept H_1 when $B_\alpha(f_{1\cdot}, f_{2\cdot}; f_{T\cdot}) \geq 0$, where

$$B_\alpha(f_{1\cdot}, f_{2\cdot}; f_{T\cdot}) = e_\alpha(f_{2\cdot}, f_{T\cdot}) - e_\alpha(f_{1\cdot}, f_{T\cdot}) \tag{8}$$

and

$$e_\alpha(f_{j\cdot}, f_{T\cdot}) = \frac{1}{2} \sum_{k=0}^{T-1} \left\{ \log\left(1 - \alpha + \alpha \frac{f_{j\cdot}(\nu_k)}{f_{T\cdot}(\nu_k)} \right) - \alpha \log \frac{f_{j\cdot}(\nu_k)}{f_{T\cdot}(\nu_k)} \right\}. \tag{9}$$

In terms of the overall criterion involving both phases, we would accept H_1 when

$$B_\alpha(f_{1P}, f_{2P}; f_{TP}) + B_\alpha(f_{1S}, f_{2S}; f_{TS}) \geq 0. \tag{10}$$

In order to apply the discriminant functions defined above, we need to have estimators for the earthquake and explosion spectra, say $f_{1\cdot}(\nu)$ and $f_{2\cdot}(\nu)$. These can be taken as predefined values if no training sample is available or as the averages of the earthquake and explosion spectra respectively if a training sample is available. We take the values here of the average earthquake and explosion spectra shown in Figure 2. The spectra were computed for each series (no taper) over a fairly broad band (2 Hz) and then averaged separately for earthquakes and explosions. Note that the P and S components were scaled by dividing by the maximum of the P component. For the quadratic and information theoretic detectors, small values of the theoretical spectra can cause potential distortions, so several cutoff frequencies in Equations (1), (5) and (9) were tried; overall best performance seemed to be attained with a cutoff of about 8 Hz. In Figure 1, we see that real differences in the earthquake and explosion spectra are small after this point.

The P and S components of the quadratic detector are plotted in Figure 6 and we see that both the test sample and the holdout procedures achieve perfect classification. Note that the performance of the holdout procedure emulates the performance that a

9

discriminant function defined from a training sample would have on a new observation. One computes the average of the spectra holding out one observation at a time and then using the test statistic to classify the held out observation. The events that are somewhat marginally classified since they lie somewhat close to the decision line in the hold-out sample are Earthquake 4 (Figure A4) and Explosions 1 and 8 (Figures A9 and A16).

The P and S components of the information theoretic based discriminants are shown in Figure 7 for $\alpha = .7$ and we see that the separation is slightly better for the robust ZT α-entropy than for the MDI detector whose performance is similar to that of the ordinary likelihood discriminant shown in Figure 6. Experimenting with lower values of α showed a slight degradation. It would appear that the ZT α-entropy discriminant, which is robust to peak contamination, is doing a better job in this case. Note also that the distribution of the ZT discriminant is less skewed than that of the MDI or likelihood detectors where the explosions tend to be clustered in a small region and the earthquakes tend to be distributed over a large dynamic range. The holdout performance of both detectors, shown in Figure 8, is perfect and we note that one explosion in the MDI holdout population moves quite close to the discriminant line. The marginal events might be taken as Earthquakes 4 and 5 although they are quite far from the decision line.

5. Parametric Discriminants Based on Complexity

In order to define an *optimal parametric discriminant*, consider a model for the earthquake or explosion P phase specified as a stationary autoregressive series modulated by a time varying function sometimes used for earthquake and explosion sources. That is, we assume the observed P phase is generated by

$$y_t = c_t(\Theta)x_t + v_t \tag{11}$$

where $a_t(\Theta)$ is some modulating function depending on t and the parameter vector $\Theta = (\theta_1, \theta_2, \ldots, \theta_p)'$. The process x_t is an underlying signal and its reflections and v_t is an additive white noise process. Dargahi-Noubary (1992) has suggested such a model where the modulating function might be taken as

$$a_t(\theta_1, \theta_2) = \theta_1 t \exp(-\theta_2 t) \tag{12}$$

One may motivate such modulating functions by appealing to standard source theory models such as Harkrider (1976) or Von Seggern and Blandford (1972) whose model implies

10

a source time function of the form

$$a_t(\theta_1, \theta_2, \theta_3)) = (\theta_1 t + \theta_2 t^2) \exp(-\theta_3 t).$$

The modulating function (12), suggested by Dargahi-Noubary (1992), has a shape which depends on the parameters θ_1 and θ_2. Small values of θ_1 and θ_2 should be associated with earthquakes since they produce emergent modulating functions; large values of these two parameters would characterize explosions since these larger values will produce rather impulsive waveforms. Some families of typical modulating functions obtained with this data are shown in Figure 9.

Since the modulating functions are rather smooth, the underlying process should be modeled by a random series with a fairly well defined peak spectrum. Second-order autoregressive series are useful for fitting these kinds of series and accordingly, we take the modulated process x_t as

$$x_t = \phi_1 x_{t-1} + \phi_2 x_{t-2} + w_t, \tag{13}$$

where the noise processes errors have variances σ_v^2 and σ_w^2; for identifiability, σ_w^2 should be fixed at a constant value. The second-order model implies a fall off in frequency that is inversely proportional to ν^2 which is consistent with the Von Seggern Blandford theory.

In order to get an indication as to how the model defined in (12) and (13) might work, we developed a maximum likelihood procedure for estimating the parameters $\theta_1, \theta_2, \sigma_v^2$ and ϕ_1, ϕ_2. The model is highly nonlinear in all parameters but we can write the log likelihood function of the complete data as in Shumway (1988) and then use the EM algorithm. The basic procedure is to update ϕ_1, ϕ_2 and σ_v^2 using the EM algorithm and to update θ_1 and θ_2 by Newton-Raphson interations nested within the EM algorithm.

The above procedure is quite sensitive to start points and the families of modulating functions shown in Figure 9 for earthquakes and explosions are not clear emergent and impulsive as they should be. The scatter plots of the parameters ϕ_2, ϕ_2 and θ_1, θ_2 are shown in Figure 10 and again there is a clear separation only relative to θ_1 which is proportional to the P/S amplitude ratio. This happens because the amplitudes of the P is scaled by dividing by the maximum amplitude of the S phase for that event. A discriminant analysis using the parameters θ_1 and θ_2 lead to misclassifying Earthquakes 2 and 8 and Explosions 4 and 5. Note in Figure 5 that these are the events that one sould expect to misclassify on the basis of the estimating modulating functions. Looking at the original events, it is reasonable that Explosions 4 and 5 would be fitted well by emerging modulators but the emergent behavior of Earthquakes 2 and 8 would seem to contradict

their fitted waveforms. It is plausible that the estimation procedure could be tuned to the process by comparing against envelope functions starting from a fixed time point for the maximum excursion and we are in the process of testing this method.

5. Conclusions and Recommendations

We conclude that the optimal nonparametric procedures based on spectral differences discriminate significantly better than those based on extracting simple features of the process or on fitting the amplitude modulated model for complexity. Of course, these results are only for the very small and carefully selected learning sample of Scandinavian earthquakes and explosions considered in this study. Hence, the data are not sufficient to give confidence from a discrimination point of view but they are adequate to indicate the potential of the new statistical methods. It is of potential interest also to develop a method for incorporating a third *noise-only* hypothesis into the decision procedure in order to decide whether there is significant signal/noise to justify a discrimination.

The advantage of the nonparametric procedures based on *likelihood, minimum discrimination information* and α-*entropy* essentially relate to their ability to tune against all differences present in the earthquake and explosion spectra and not to specific frequency bands or phases. Furthermore, the α-*entropy* modification seems to be a promising robust technique in this case where there can be interfering or slightly offset peaks in the sample spectrum associated with the event to be classified. In addition, for more realistic larger samples and more than one station used per event, the procedure can work even better. The application of the nonparametric procedure to larger data bases should provide some standard baseline statistics for comparison with more esoteric nonlinear methods such as classification trees or neural nets as applied to specific feature vectors.

The modeling of complexity using the waveform model proposed here may also add discrimination capability for the cases where the spectral matching function given by the nonparametric procedure is not enough. We will continue to refine the properties of the waveform comparison test and apply it to the small test sample of Scandinavian events.

REFERENCES

Alagon, J. (1989). Spectral discrimination for two groups of time series. *J. Time Series Analysis*, **10**, 203-214.

Blandford, R.R. (1981). Seismic discrimination at regional distances. In *Identification of Seismic Sources- Earthquake or Underground Explosions*. Ed. by E.S. Husebye and S. Mykkeltveit, D. Reidel Publishing Co, 695-740.

Blandford, R.R. (1985). Regional detection, location, discrimination and yield determination. In *The VELA Program*, Ann Kerr, Ed. 787-816, Executive Graphic Services 85-080931, 787-816.

Blandford, R.R. (1993). Discrimination of earthquakes and explosions at regional distances using complexity. Presented at Air Force Technical Applications Review, Patrick AFB, Feb. 16-17, 1993.

Bennett, T.J. and J.R. Murphy (1986). Analysis of seismic discrimination capabilities using regional data from western U.S. events. *Bull. Seismolog. Soc. Amer.*, **76**, 1069-1086.

Dargahi-Noubary, G.R. and P.J. Laycock (1981). Spectral ratio discriminants and information theory. *J. Time Series Analysis*, **2**, 71-86.

Dargahi-Noubary, G.R. (1992). Models for seismic records; Why uniformly modulated ARMA? *Soil Dynamics and Earthquake Engineering*, **11**, 381-384.

Dysart, P. and J.J. Pulli (1990). Regional seismic event classification at the NORESS array: Seismological measurements and the use of trained neural networks. *Bull. Seismolog. Soc. Am*, **80**, 1910-1933.

Harkrider, D.G. (1976). Potentials and displacements for two theoretical seismic sources. *Geophys. J. R. Astro. Soc.*, **47**, 97-133.

Kim, W-Y, D.W. Simpson and P.G. Richards (1992). Discrimination of regional earthquakes and explosions in eastern U.S. using high-frequency data. Lamont-Doherty Earth Observatory, Columbia University. Preprint.

Kullback, S. (1978). *Information Theory and Statistics*. Gloucester, MA: Peter Smith.

Lachenbruch, P.A. and M.R. Mickey (1968). Estimation of error rates in discriminant analysis. *Technometrics*, **10**, 1-11.

Parzen, E. (1990). Time series, statistics and information. *IMA Preprint Series, No 663*, Institute for Mathematics and Its Applications, University of Minnesota, Mineapolis, MN 55455.

Pulli, J.J. and P.S. Dysart (1992). Neural network processing of seismic signal parameters for small event identification. Presented at the *14th Annual PL/DARPA Seismic Research Symposium*, September 16-18, Tucson, AZ, Radix Systems, Inc., 201 Perry Parkway, Gaithersburg, MD 20877.

Shumway, R.H. (1982). Discriminant analysis for time series. In *Handbook of Statistics, Vol. 2, Pattern Recognition and Reduction of Dimensionality*, ed. P.R. Krishnaiah, 1-43. Amsterdam: North Holland.

Shumway, R.H. (1988). *Applied Statistical Time Series Analysis*, Chapter 5. Englewood Cliffs: Prentice-Hall.

Shumway, R.H. and R. Blandford (1974). An examination of some new and classical short period discriminants. *Seismic Data Analysis Center, Report No. TR-74-10*, P.O. Box 334, Alexandria, VA.

Shumway, R.H. and A.N. Unger (1974). Linear discriminant functions for stationary time series, *J. Amer. Statist. Assoc.*, **69**, 948-956.

Taylor, S.R., M.R. Denny, E.S. Vergino and R.E. Glaser (1989). Regional discrimination between NTS explosions and western U.S. earthquakes (1989). *Bull. Seismolog. Soc. Amer.*, **79**, 1142-1176.

Tjøstheim, D (1975). Autoregressive representation of seismic P-wave signals with an application to the problem of short- period discriminants. *Geophys. J. R. Astro. Soc.*, **43**, 269-291.

Von Seggern, D. and R. Blandford (1972). Source time functions and spectra of underground nuclear explosions, *Geophysical J. R. Astro. Soc.*, **31**, 83-97.

Zhang, T. and M. Taniguchi (1992). Discriminant analysis for stationary vector time series. *Technical Report*, Department of Mathematical Sciences, Faculty of Engineering Science, Osaka University, Toyonaka 560, Japan.

Zhang, T. and M. Taniguchi (1993). Discriminant analysis for stationary time series. Presented at U.S.-Japan Seminar on Statistical Time Series Analysis, Jan. 25-29, 1993, Honolulu.

16

Figure 1: A well defined earthquake and explosion (Top Panel) and the extracted P and S components below. The sampling interval is .025 seconds (40 Hz). Note the emergent earthquake P and the impulsive explosion P and the relative amplitudes of the P and S components.
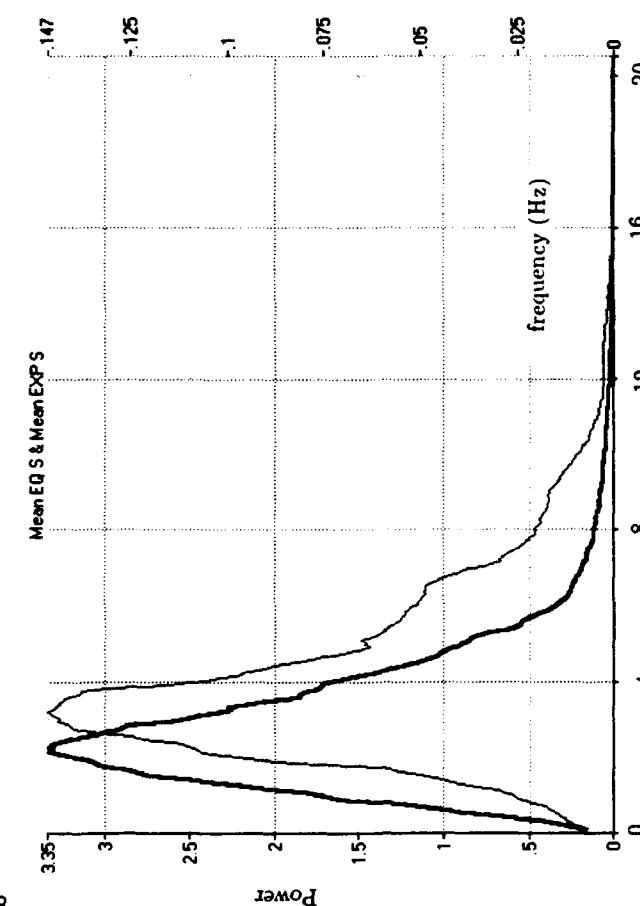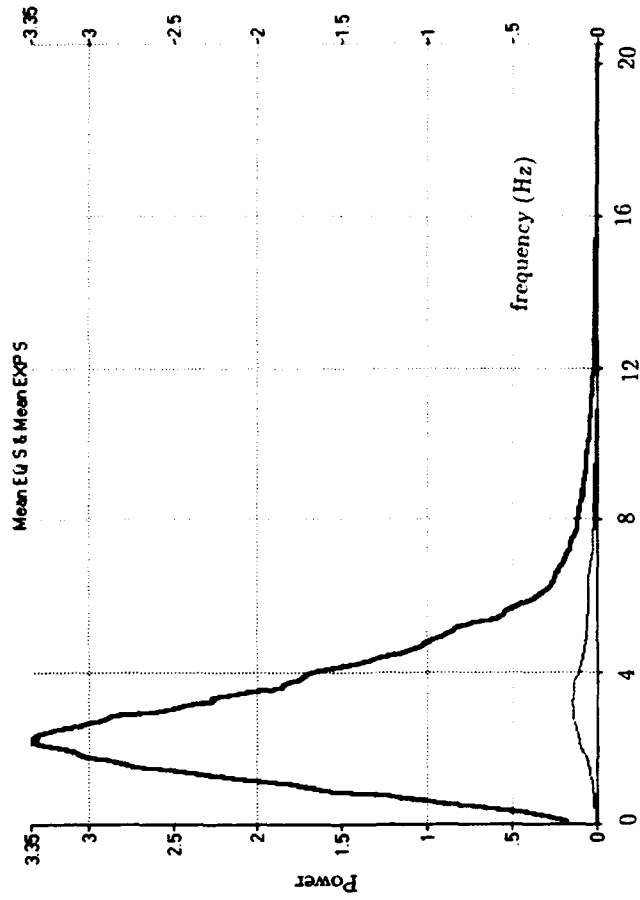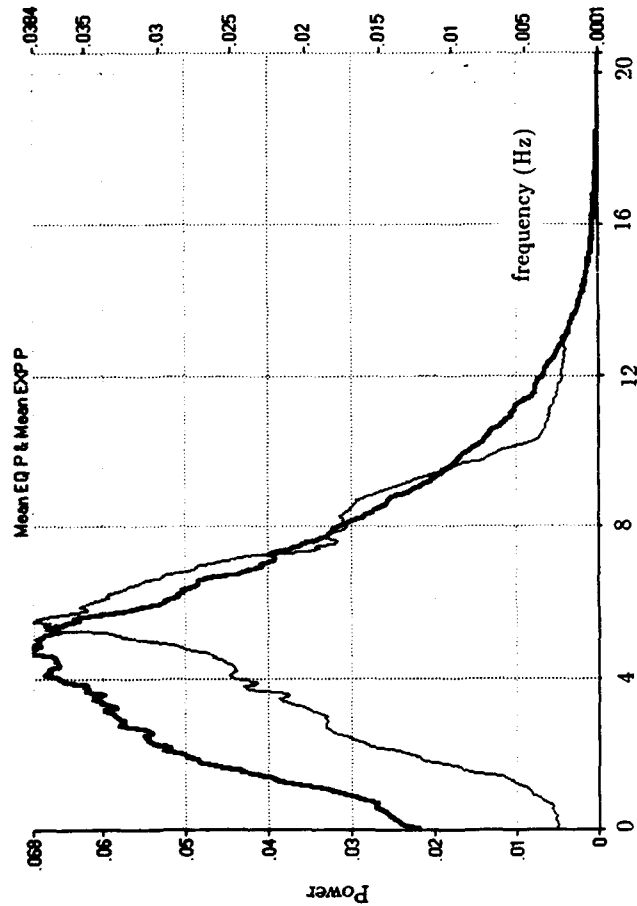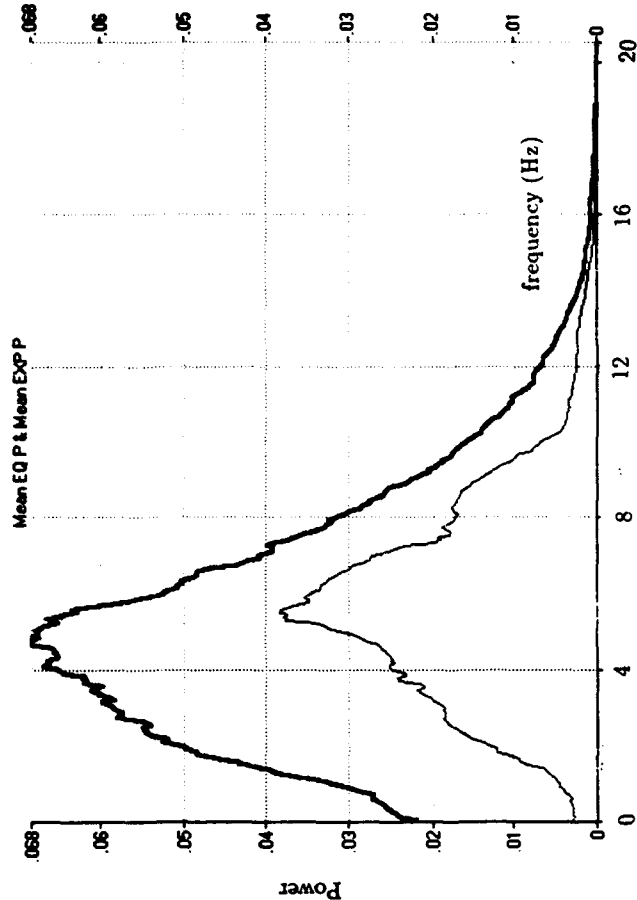
Figure 2: Average Earthquake and Explosion Spectra. The folding frequency is 20 Hz (.5 cycles per point). The darker line (left panel) is for earthquakes and the lighter line is for explosions. The right panel shows the spectra plotted on the same scale.

18
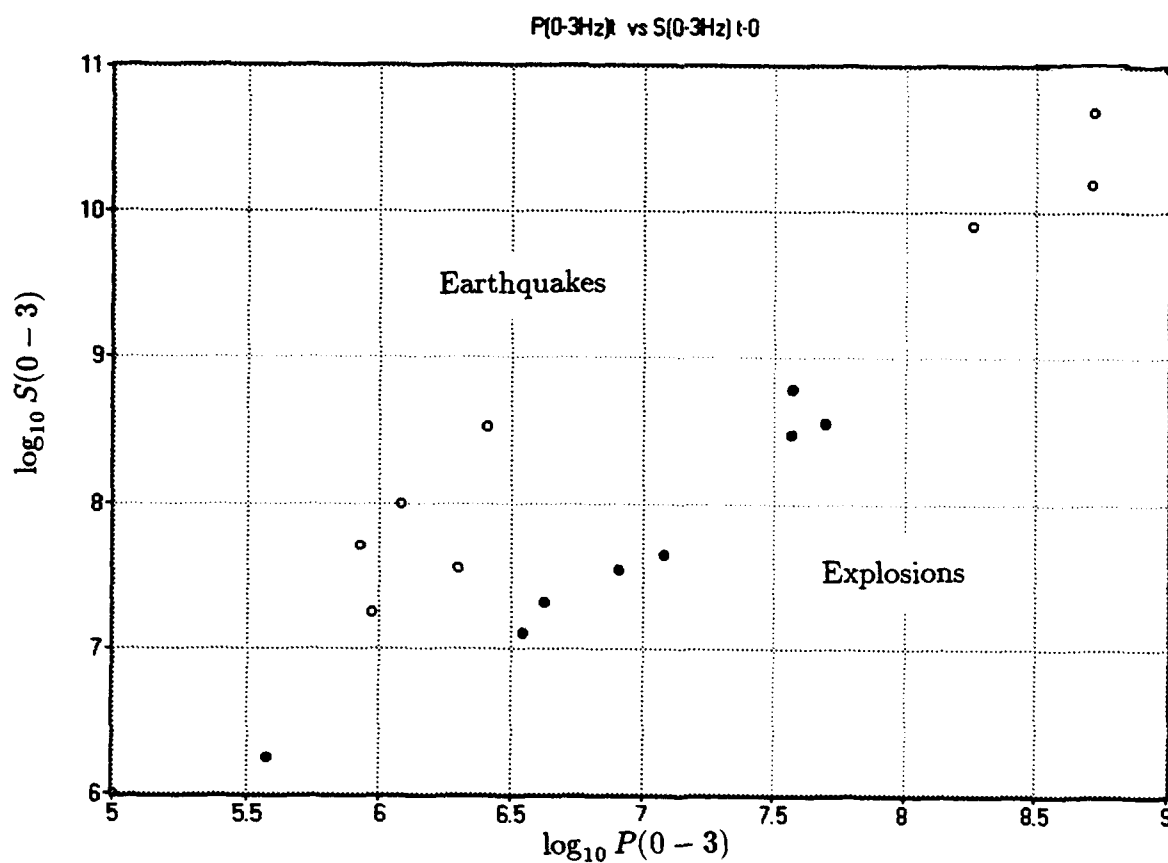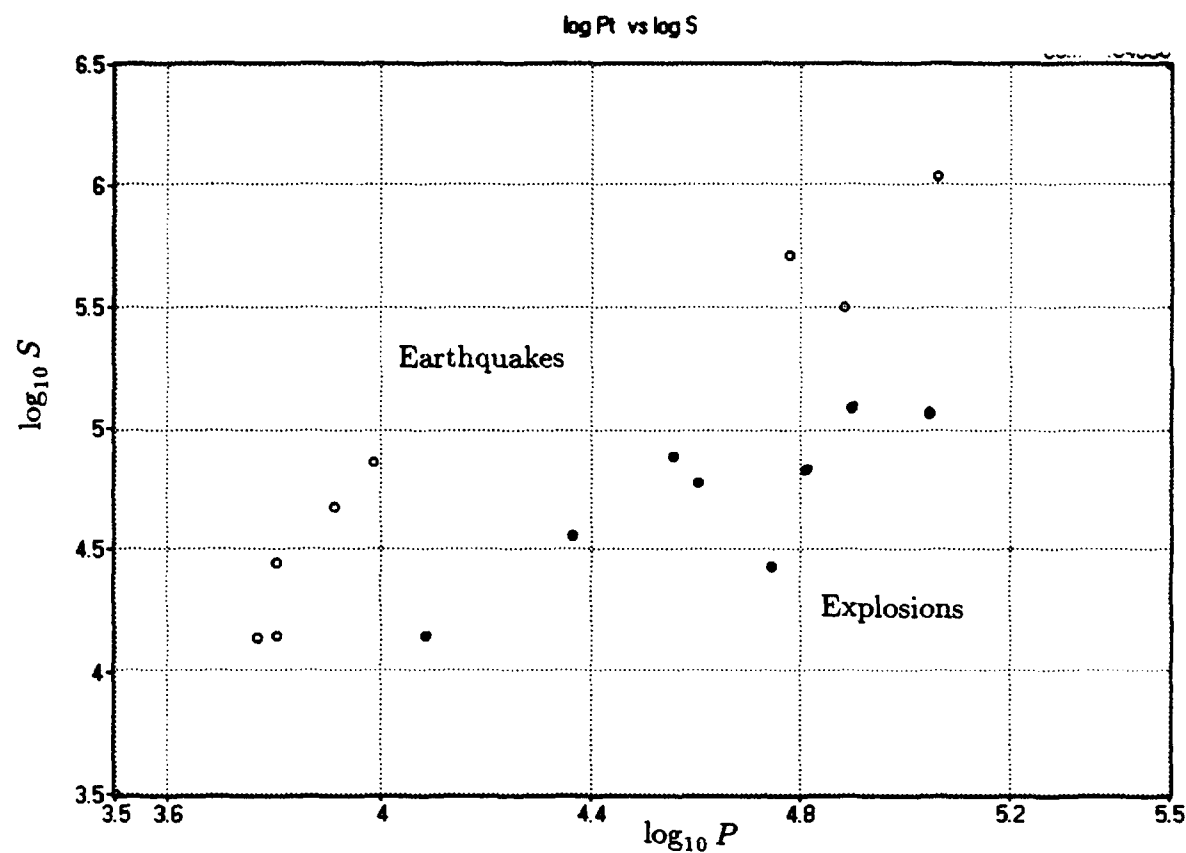
Figure 3: Scatter diagrams showing the separation between earthquakes (open circles) and explosions (solid circles) for log amplitudes of P and S (top panel) and log spectra from 0-3 Hz (bottom panel).

19

log P (0-2)t vs log P (2-4) t-0

log S (0-2)t vs log S (2-4) t-0
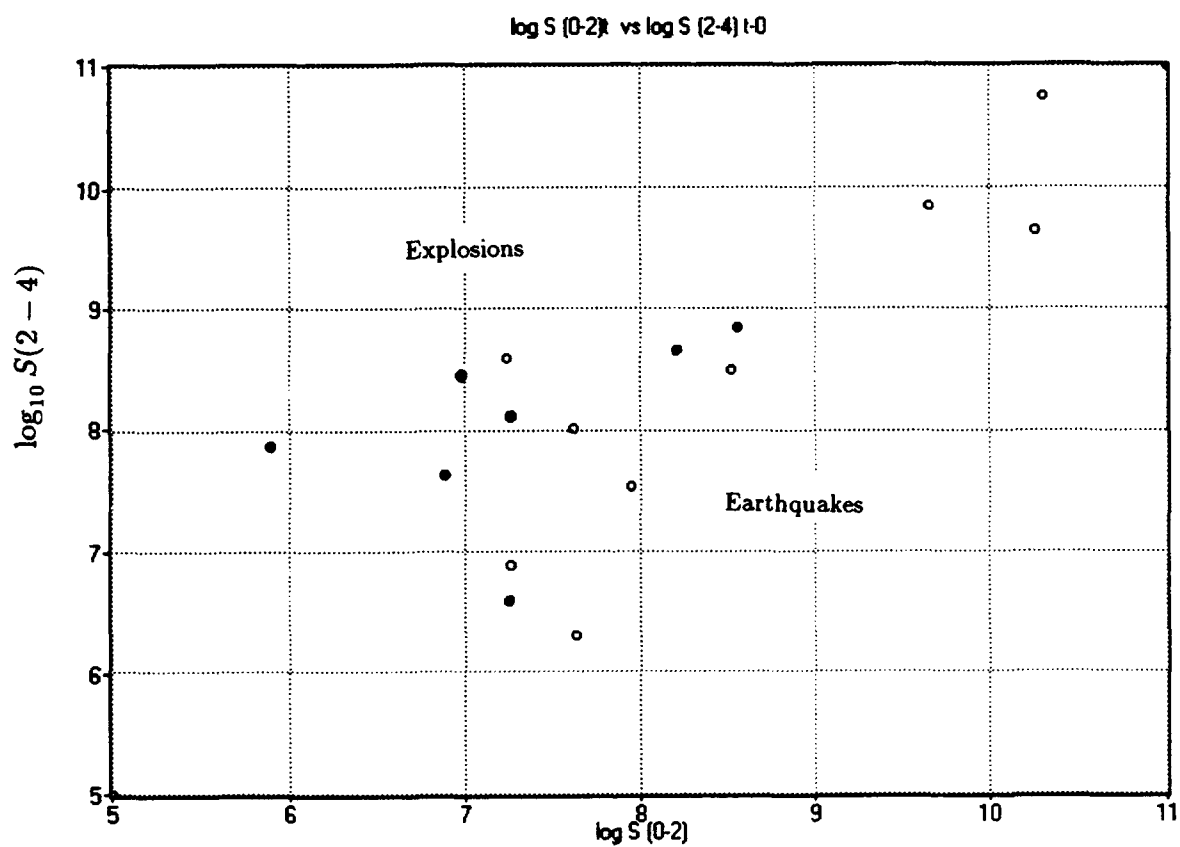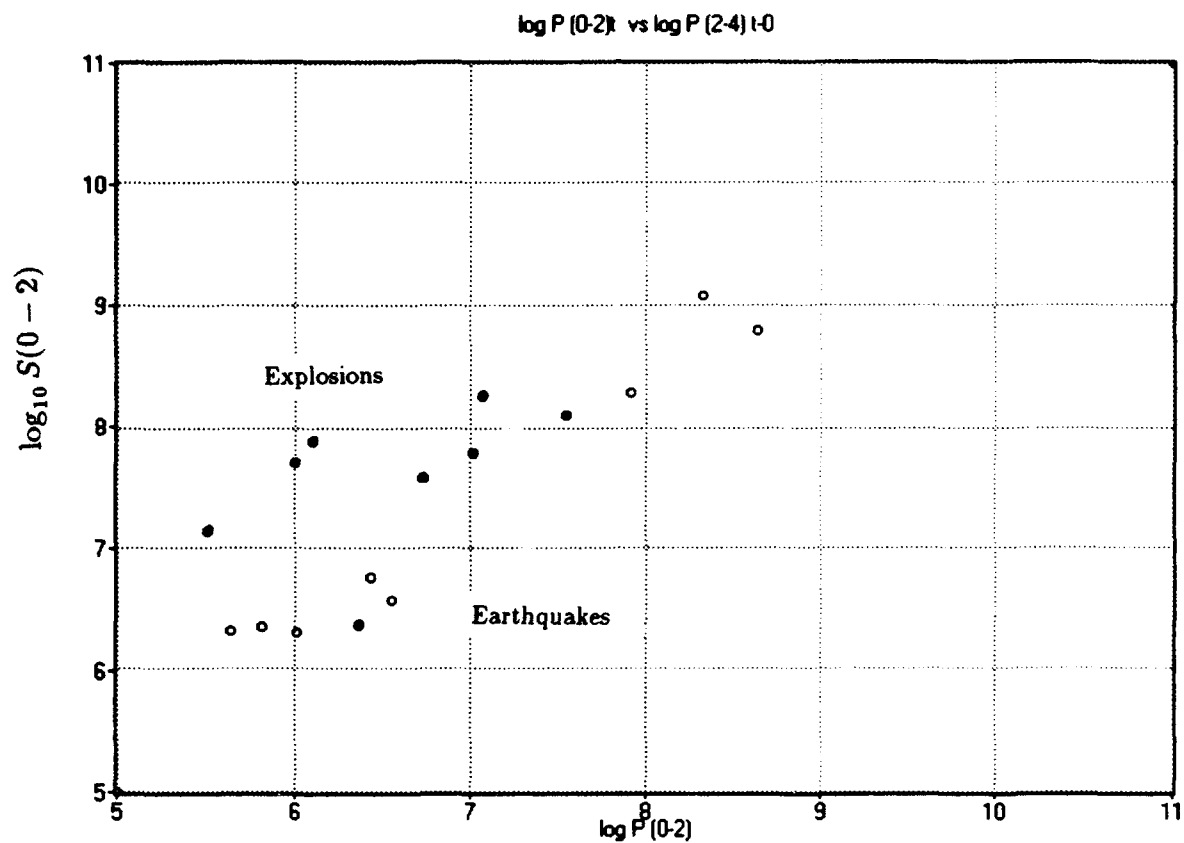
Figure 4: Scatter diagrams showing the separation between earthquakes (open circles) and explosions (solid circles) for log spectra of P(0-2 Hz vs 2-4 Hz) and S(0-2 Hz vs 2-4 Hz).

20

P(6-9Hz)t vs S(6-9Hz) t-0

log S (0-3)t vs log S (3-6) t-0
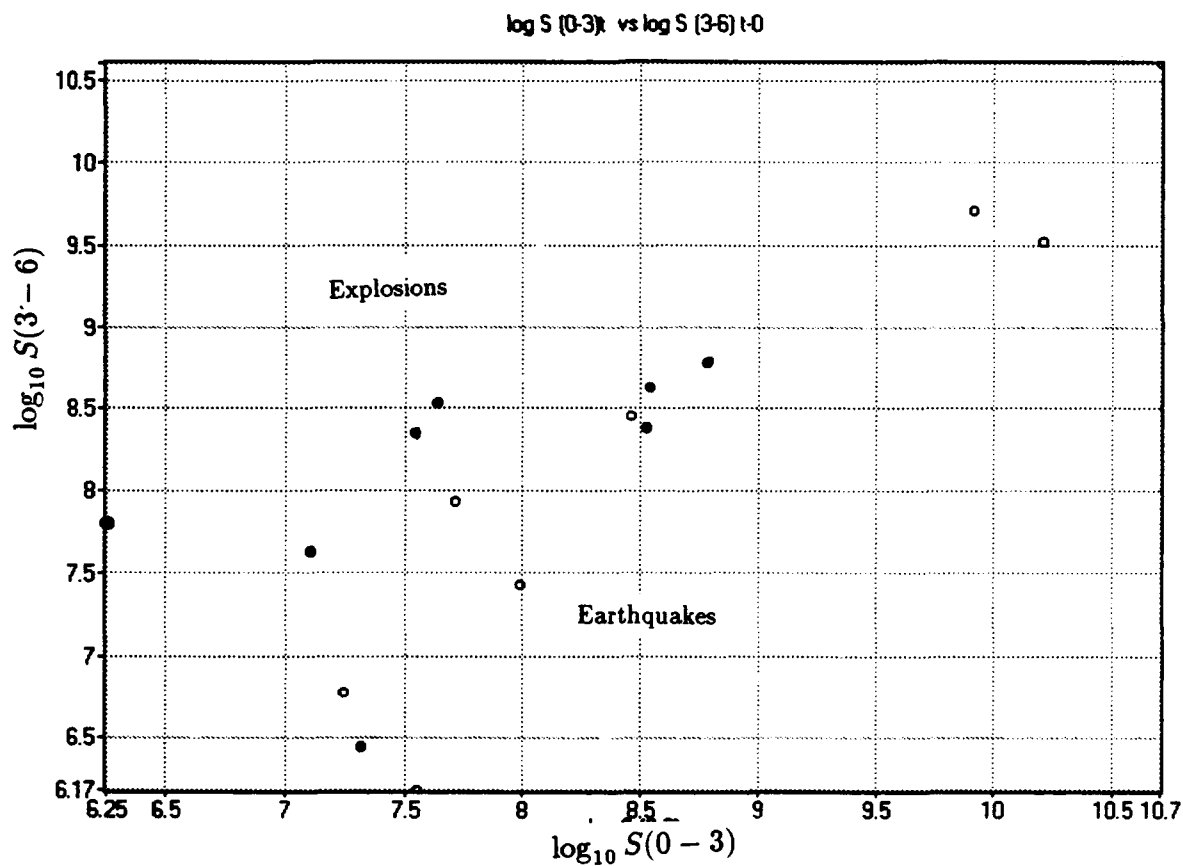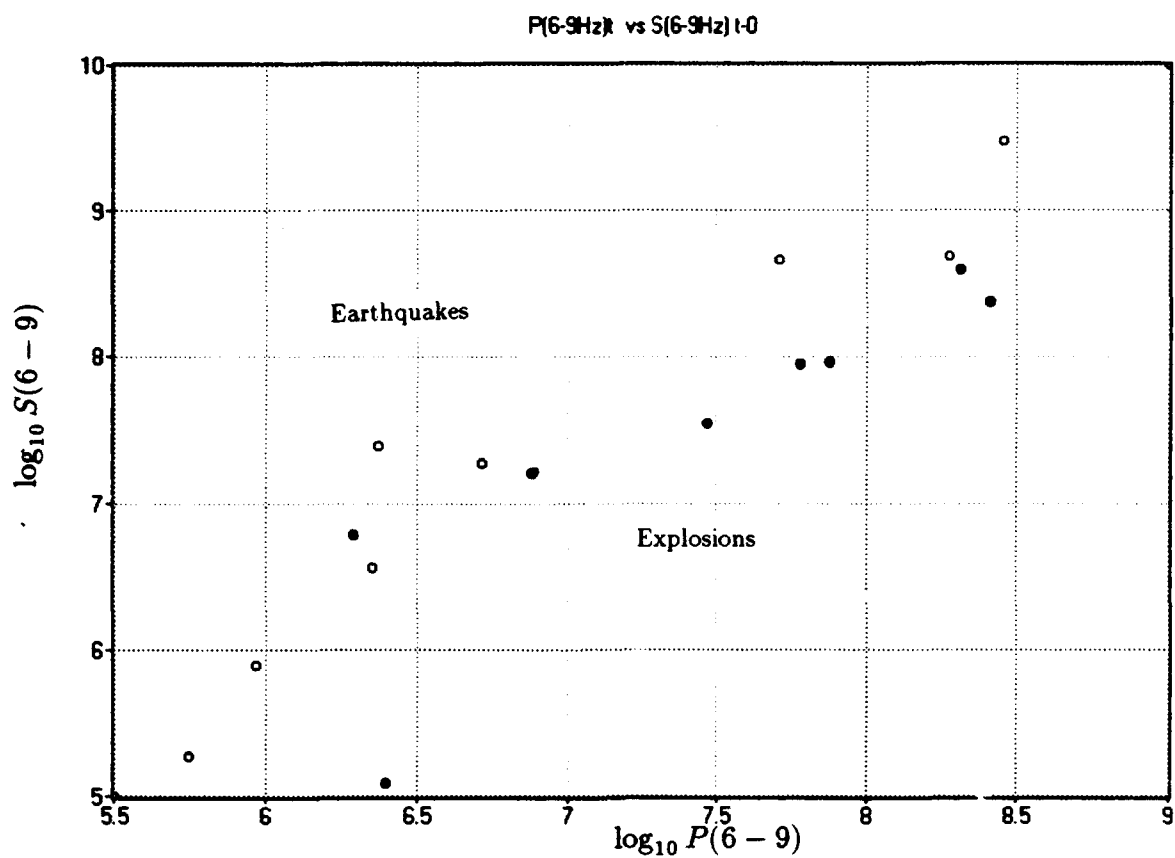
Figure 5: Scatter diagrams showing the separation between earthquakes (open circles) and explosions (solid circles) for log spectra of P(6-9 Hz) vs S(6-9 Hz) and S(0-3 Hz vs 3-6 Hz).
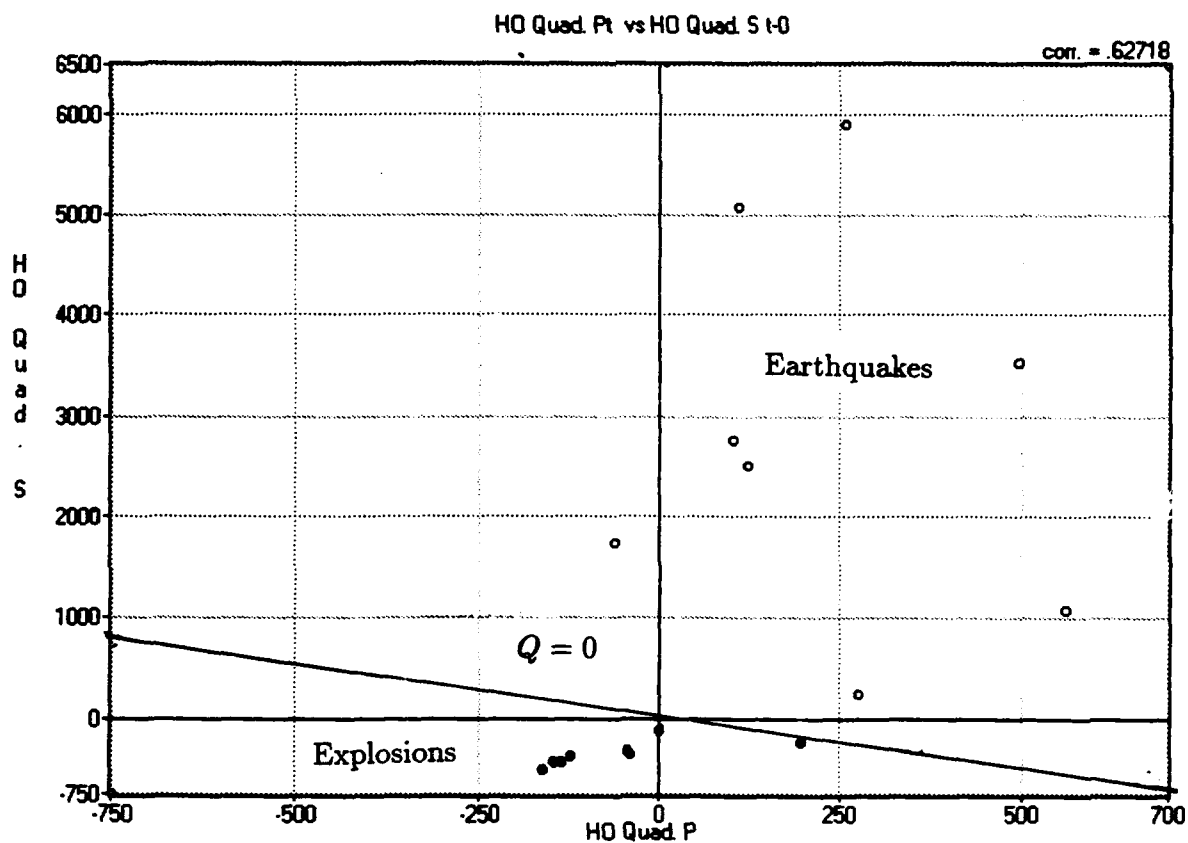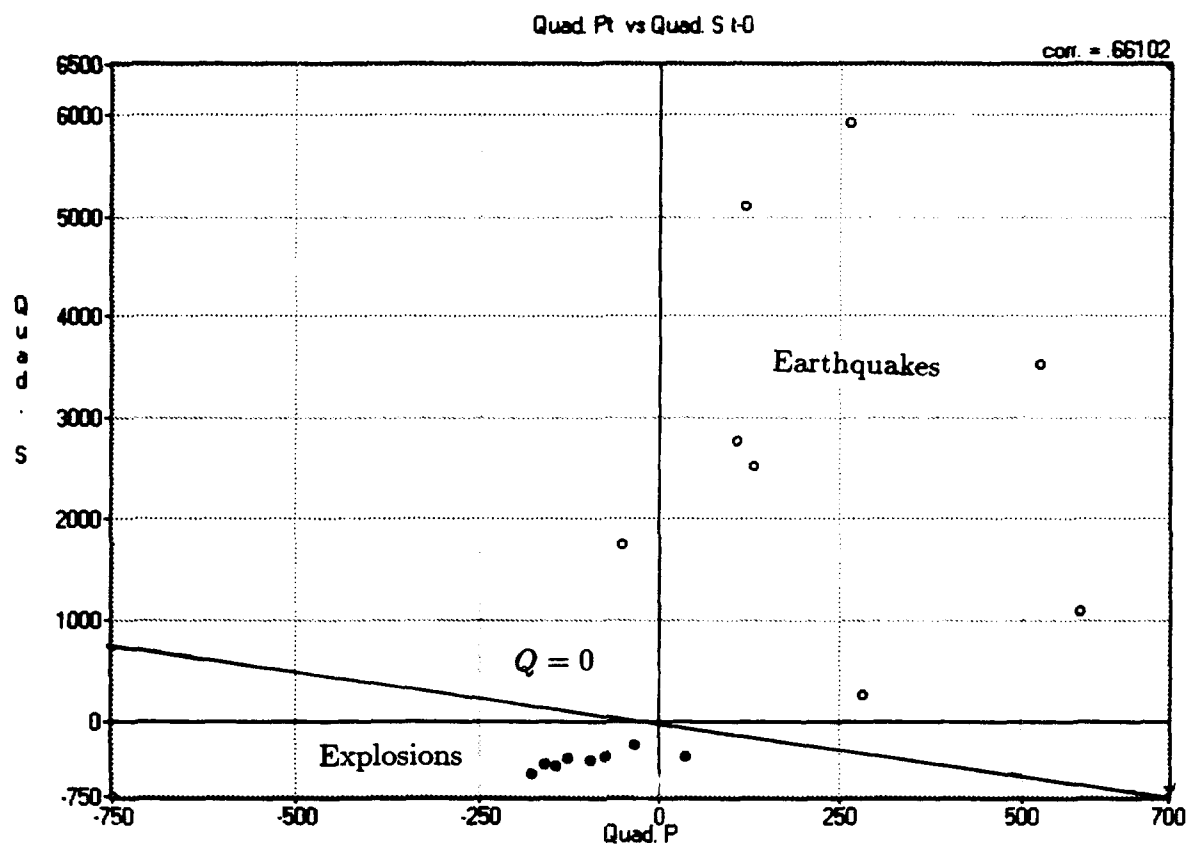
Figure 6: Separation achieved for earthquakes (open circles) and explosions (solid circles) using the optimal quadratic detector. The top panel gives the results using the learning sample whereas the bottom shows the holdout scores. The separation line $Q = 0$ is shown in both figures.
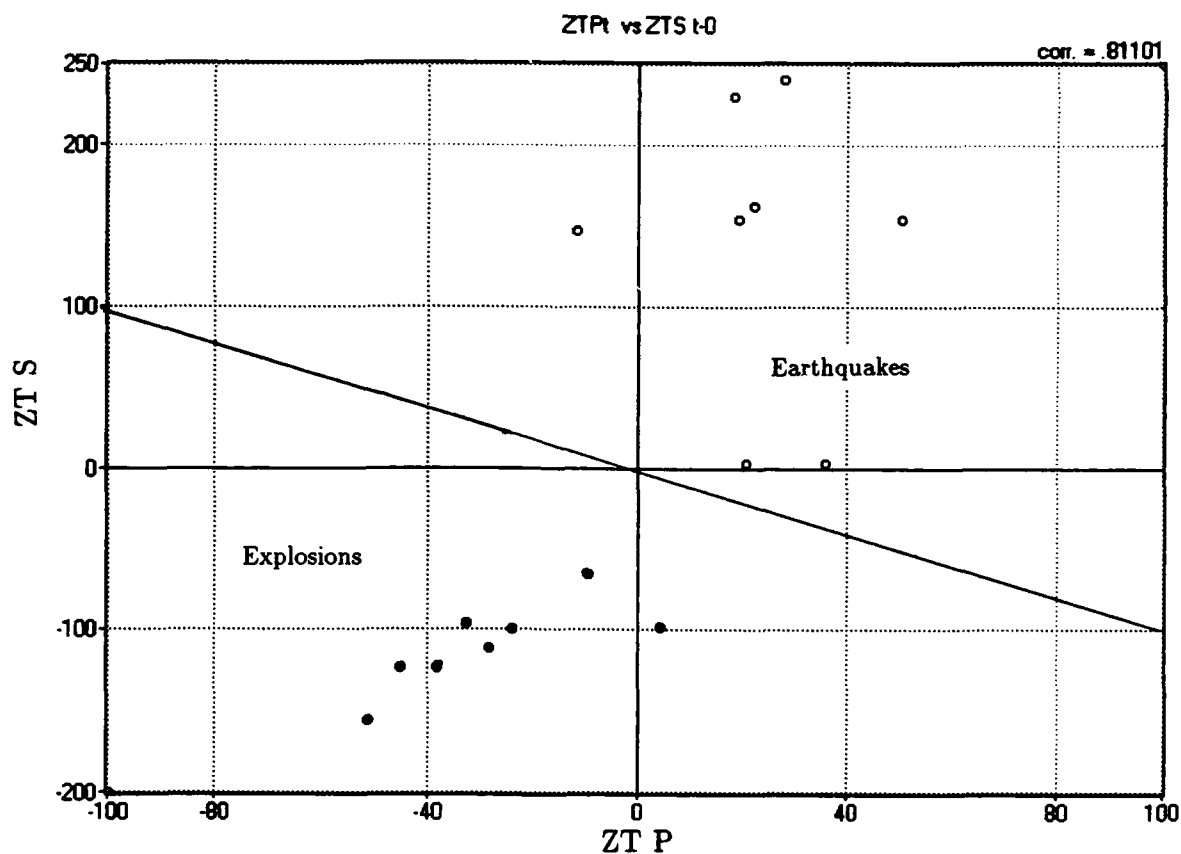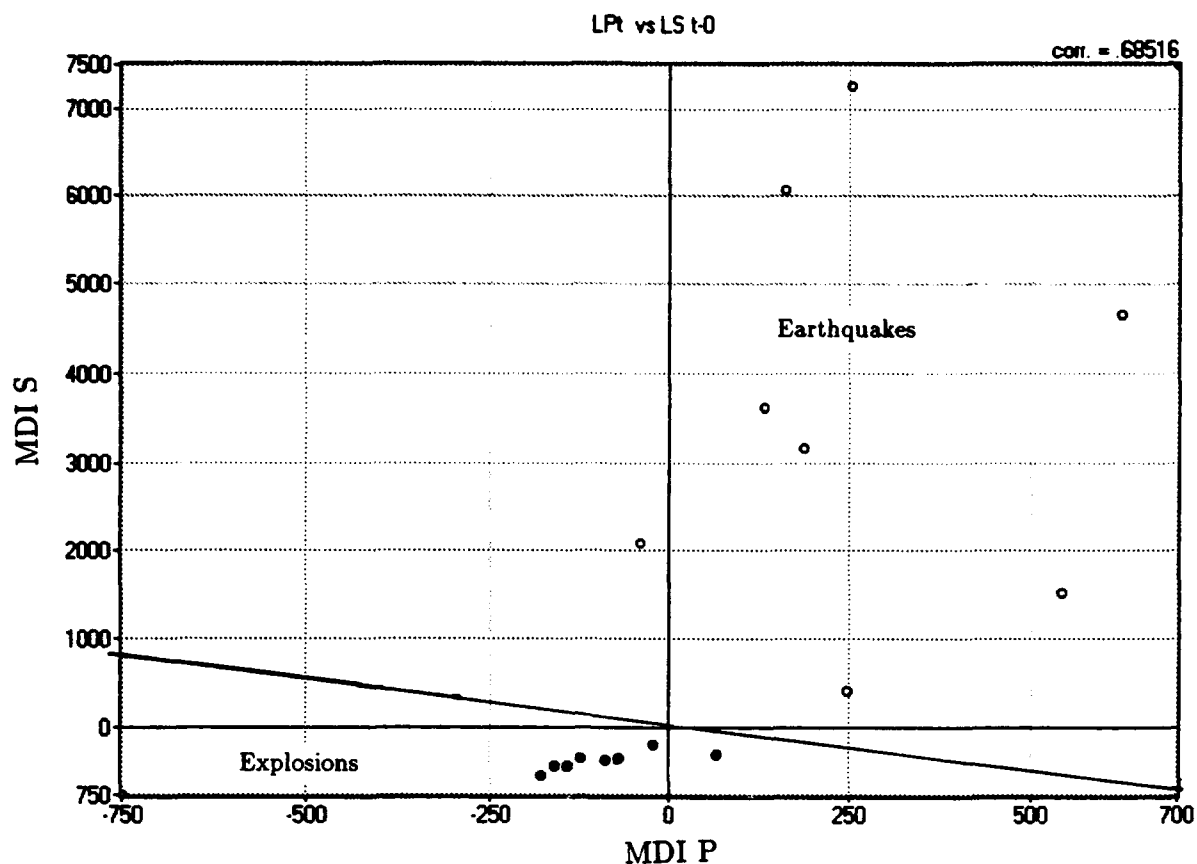
Figure 7: Separation achieved for earthquakes (open circles) and explosions (solid circles) using the *minimum discrimination information*, (MDI), (upper panel) and the Zhang-Taniguchi *α-entropy* (ZT) discrimant (lower panel) with $\alpha = .7$. The separation line $Q = 0$ is shown in both figures. Note that neither statistic misclassifies any earthquake or explosion.
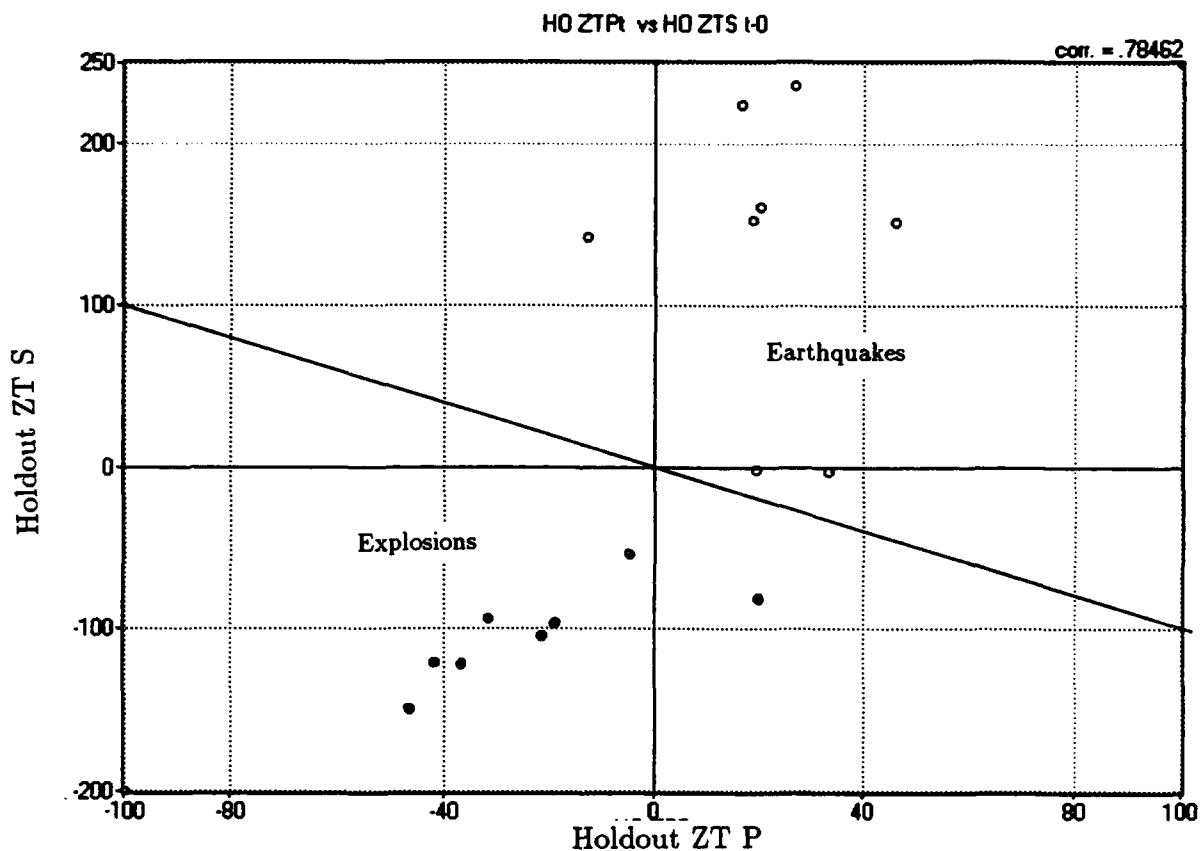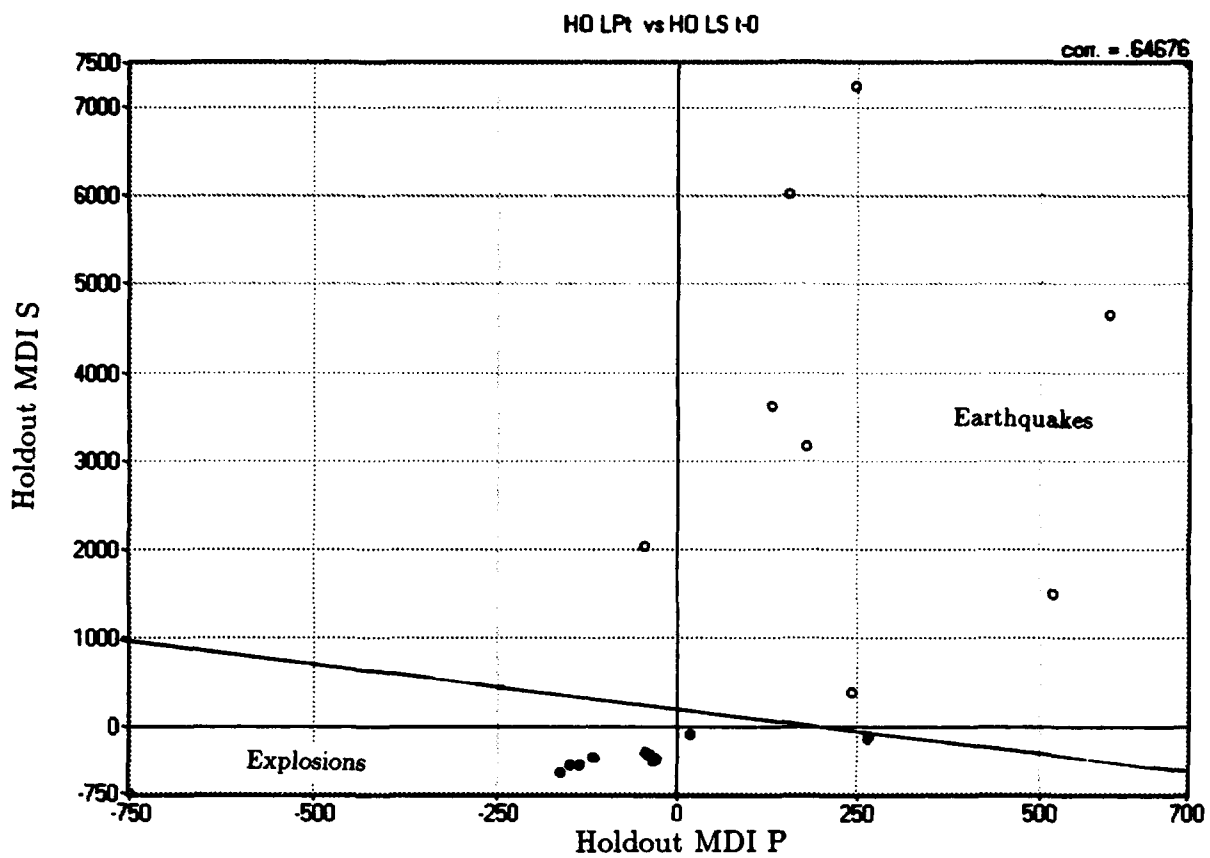
Figure 8: Separation achieved for earthquakes (open circles) and explosions (solid circles) using holdout-one versions of the MDI discriminant (upper panel) and the ZT discriminant (lower panel). The separation line $Q = 0$ is shown in both figures. Note that neither statistic misclassifies any earthquake or explosion.
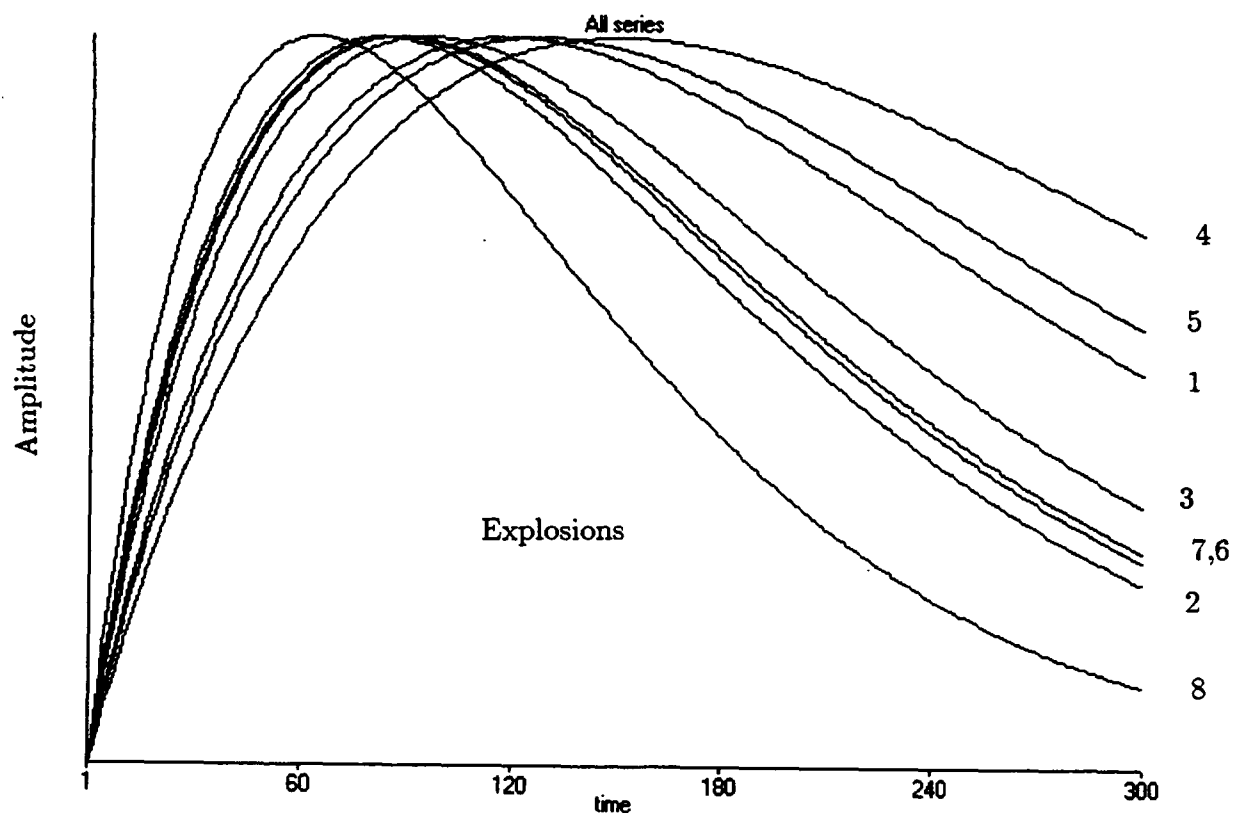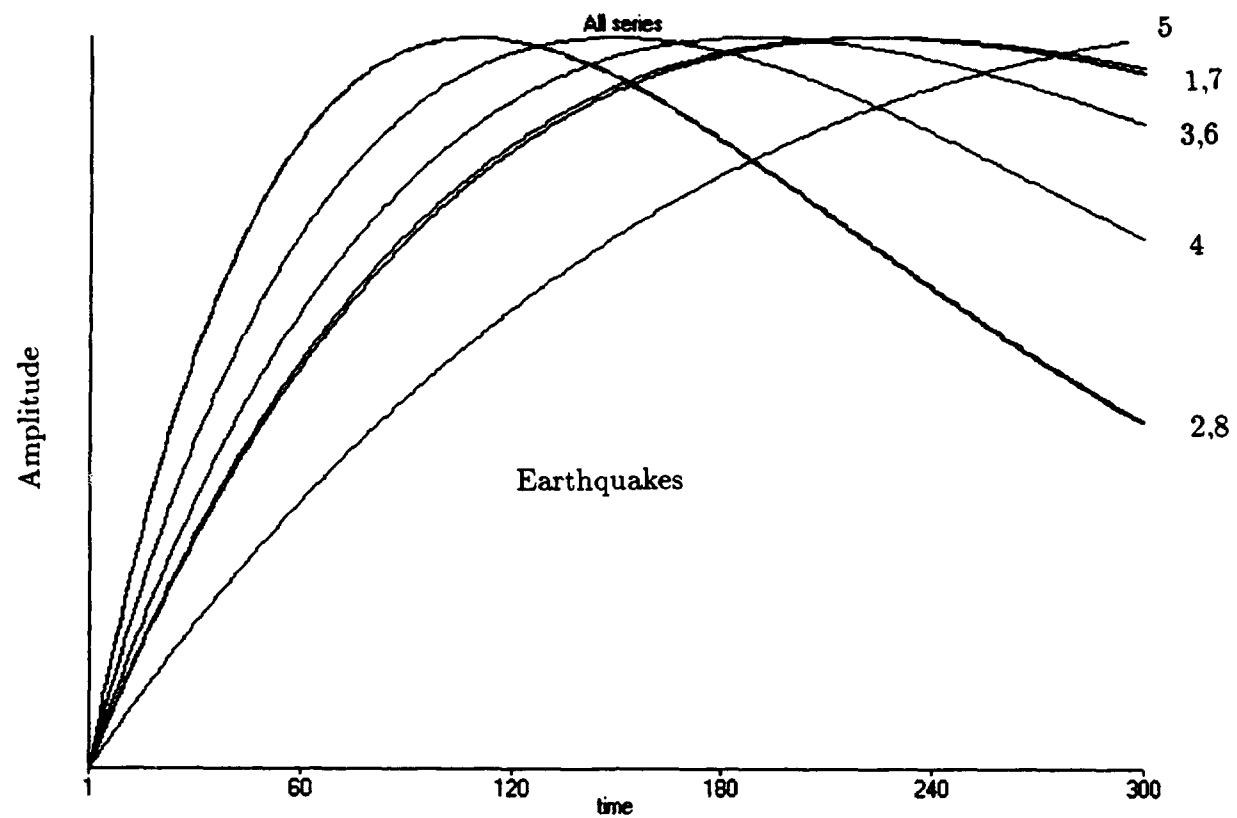
Figure 9: Plots of the estimated functions $a_t(\theta_1, \theta_2) = \theta_1 t \exp(-\theta_2 t)$ for the 8 earthquakes (Top Panel) and 8 explosions (Bottom Panel).
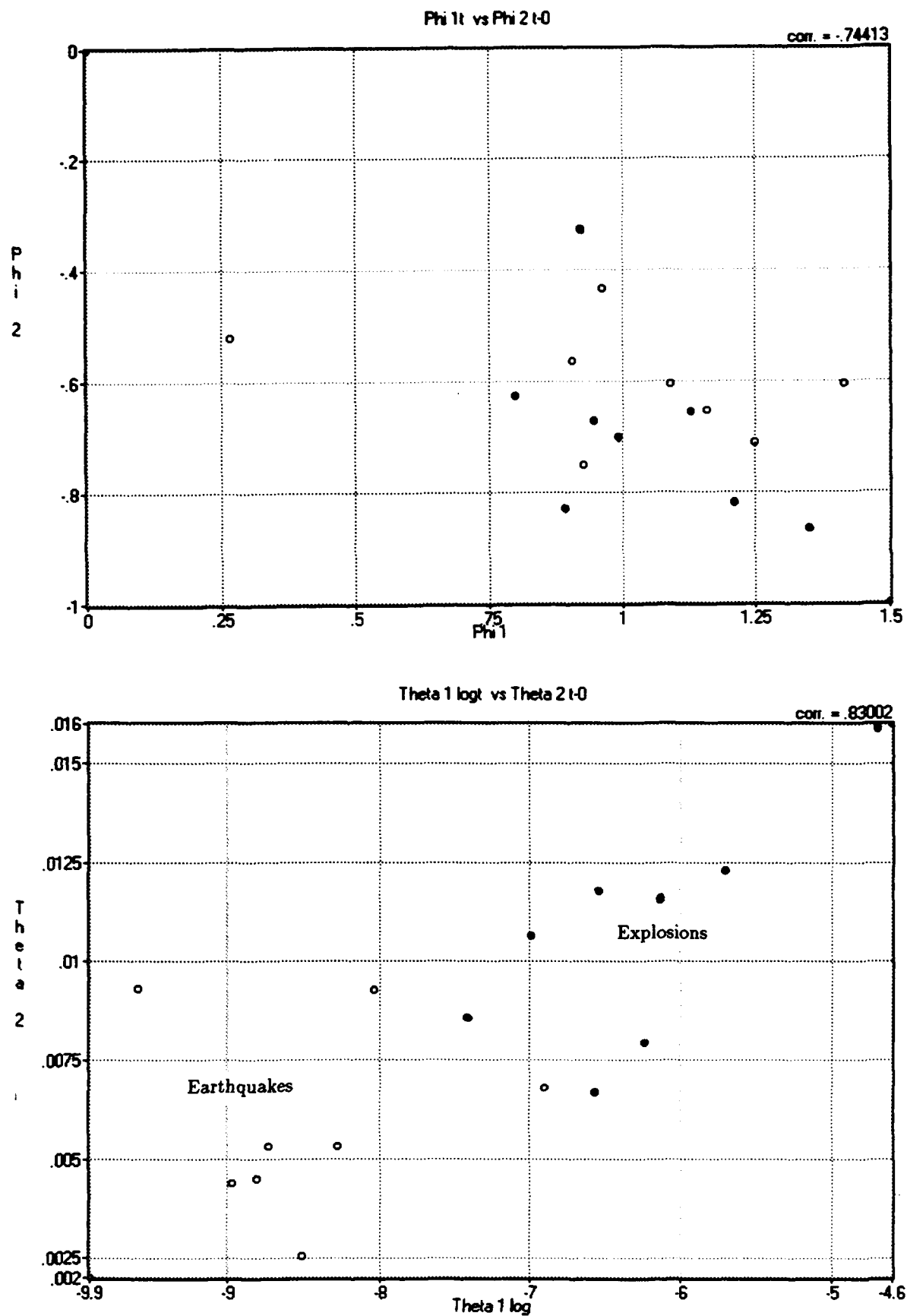
Figure 10: Scatter diagram comparing values of the parameters ϕ_1, ϕ_2 corresponding to the autoregressive part of the state space model and θ_1 and $\log \theta_2$ corresponding to the modulating functions in Figure 7. Note that most of the separation is with respect to values of $\log \theta_1$ which is proportional to log-amplitude.

26
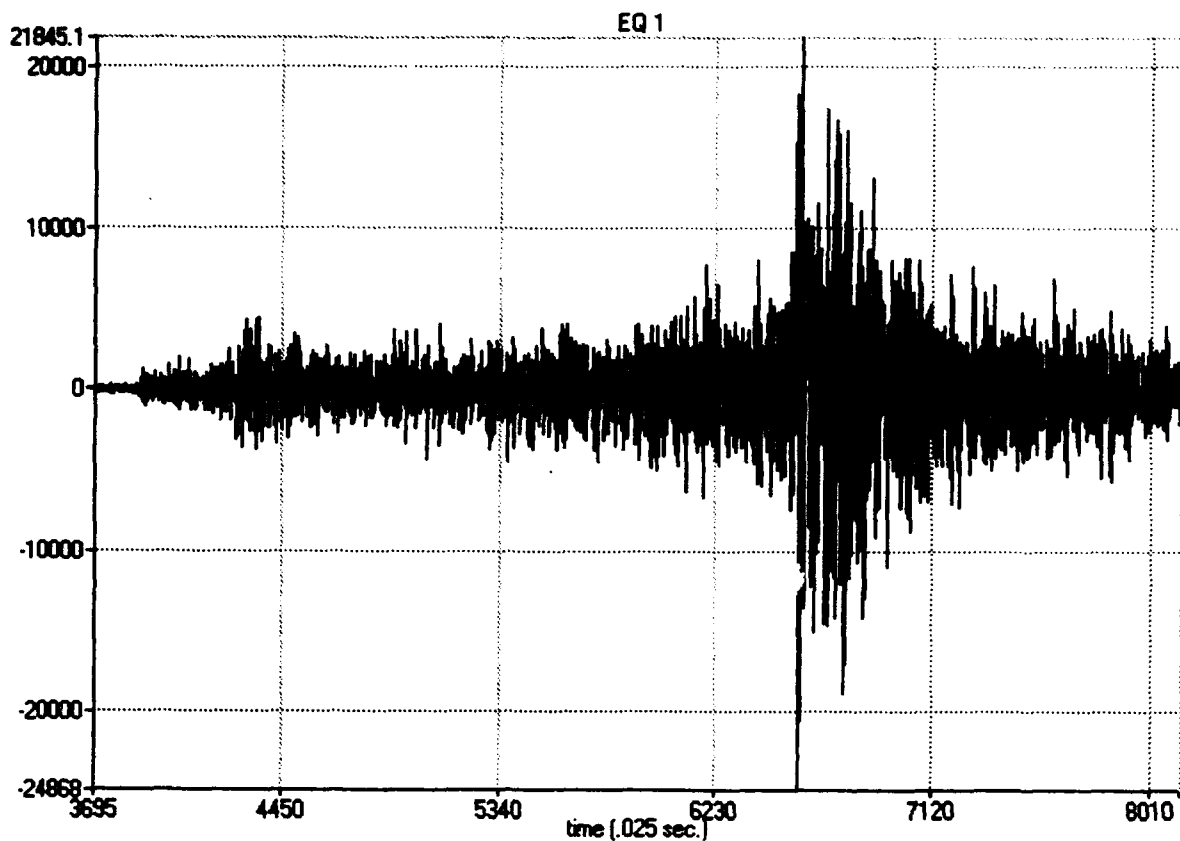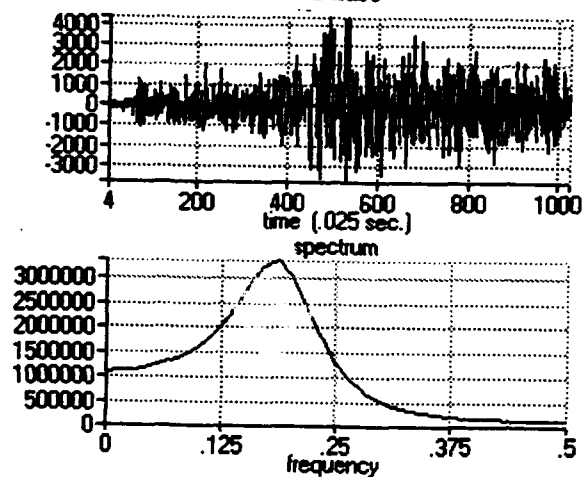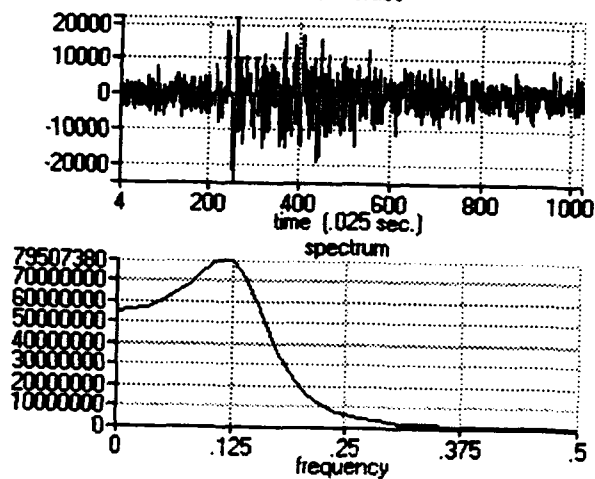
Figure A1: Earthquake 1 at Station FIA1 on 6/6/91 with local magnitude 3.22. P and S phases extracted are shown along with third-order autoregressive spectral estimators. The folding frequency is 20 Hz.

27
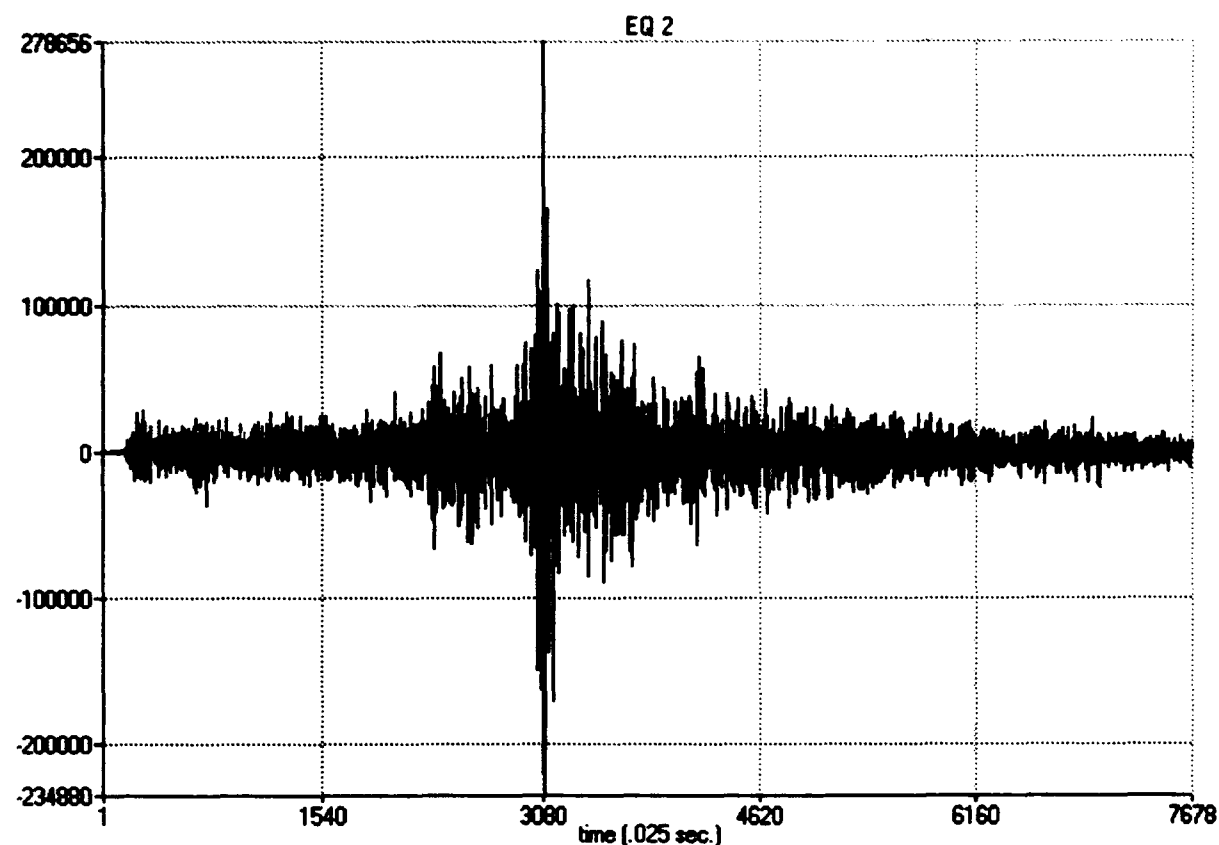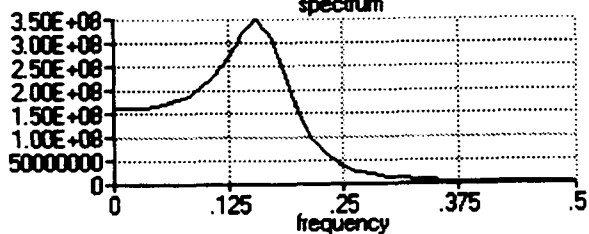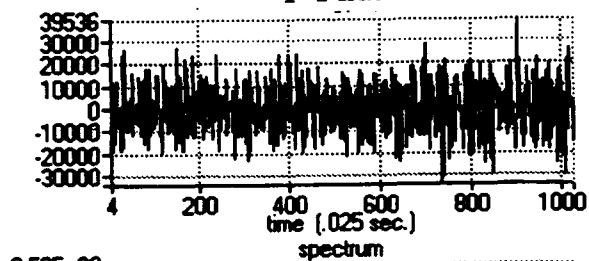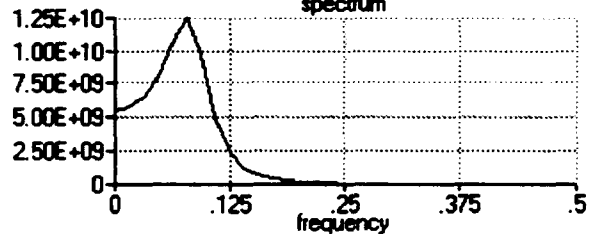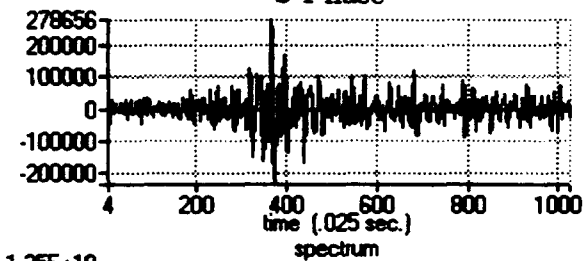
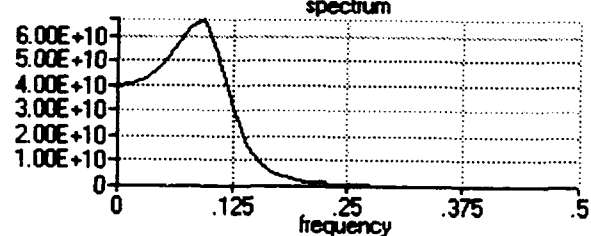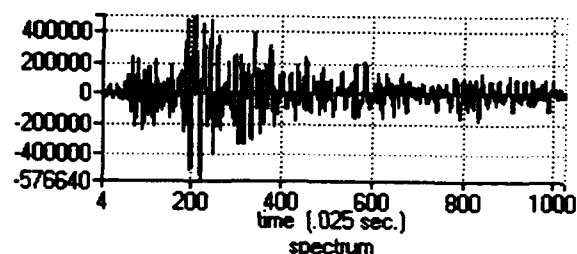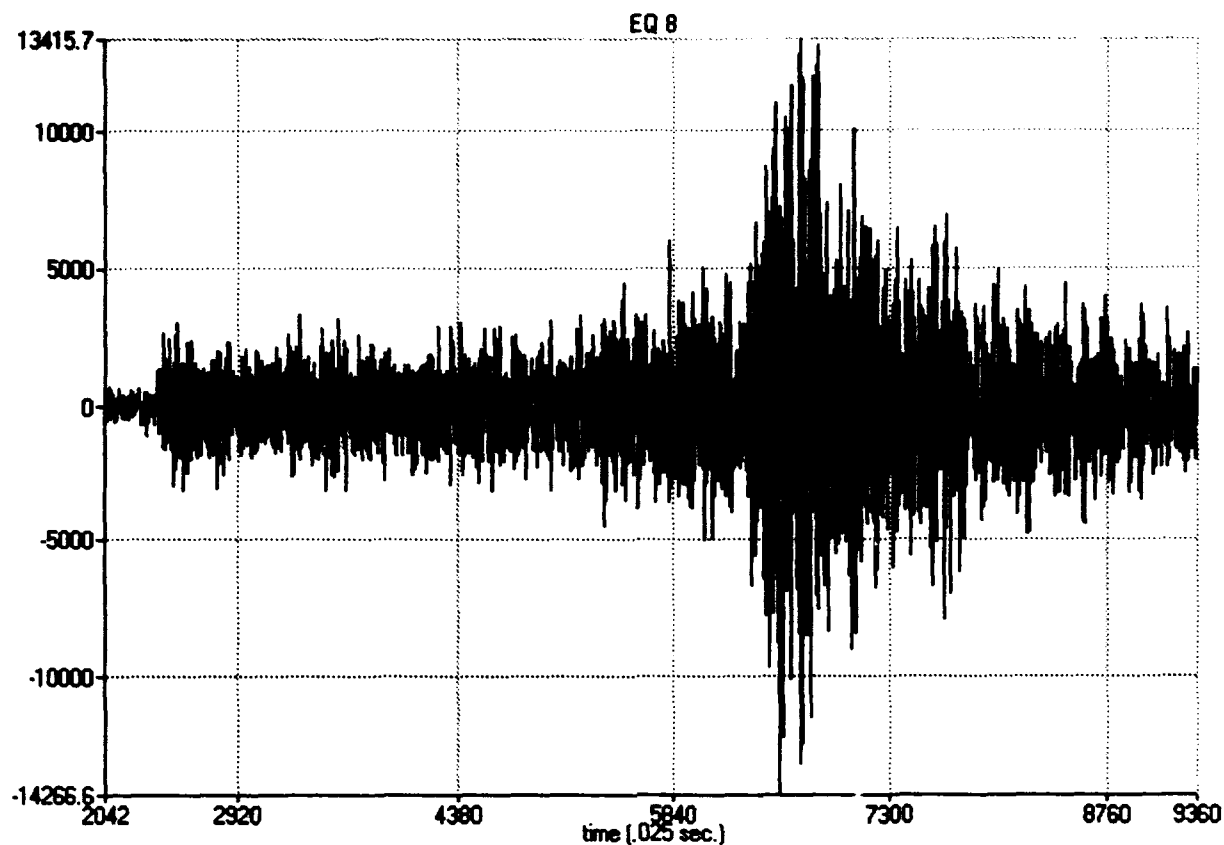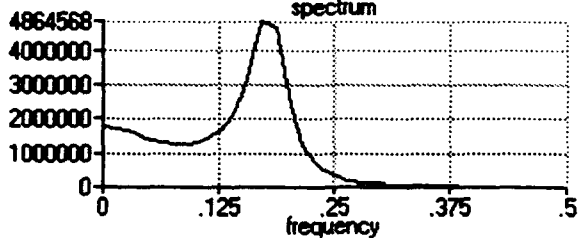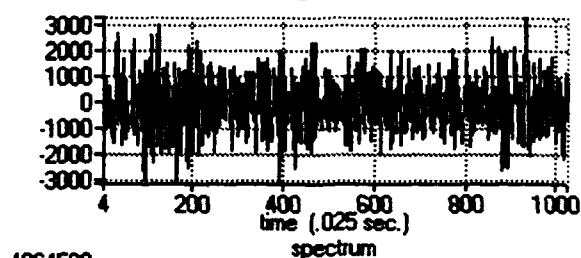Figure A2: Earthquake 2 at Station ARA0 on 8/24/91 with local magnitude 3.18. P and S phases extracted are shown along with third-order autoregressive spectral estimators. The folding frequency is 20 Hz.
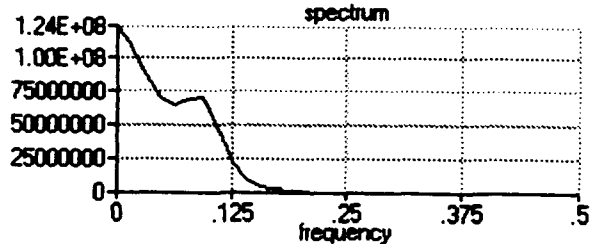
28
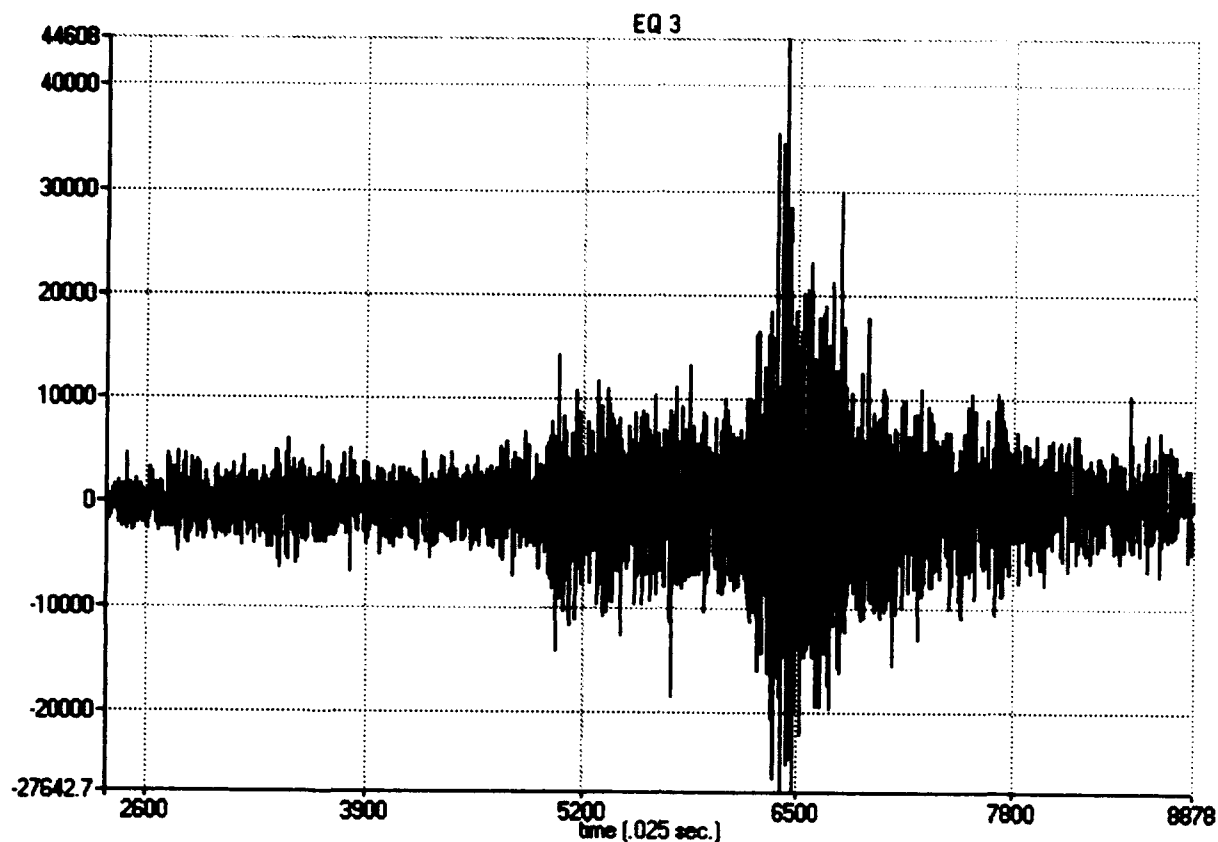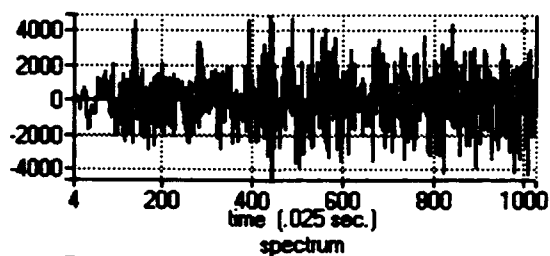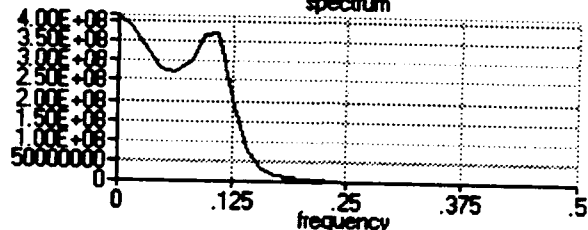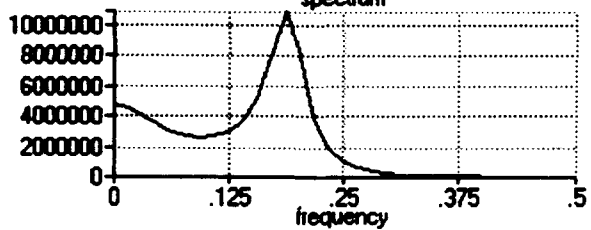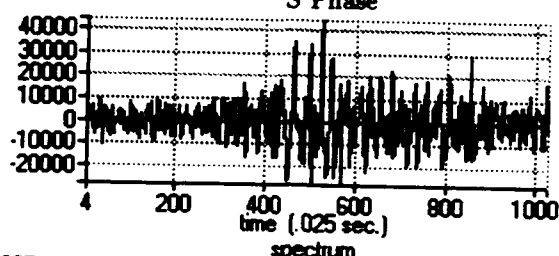
Figure A3: Earthquake 3 at Station NRA0 on 9/23/91 with local magnitude 3.15. P and S phases extracted are shown along with third-order autoregressive spectral estimators. The folding frequency is 20 Hz.
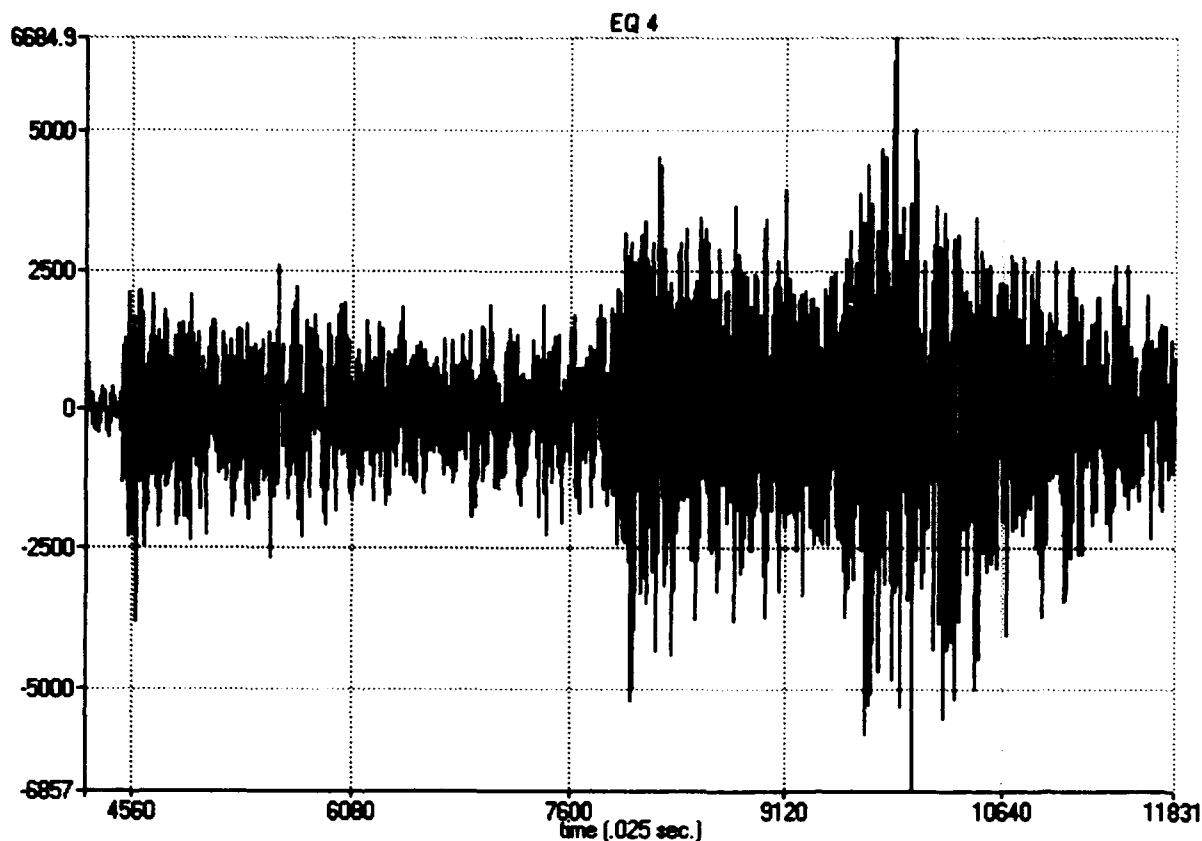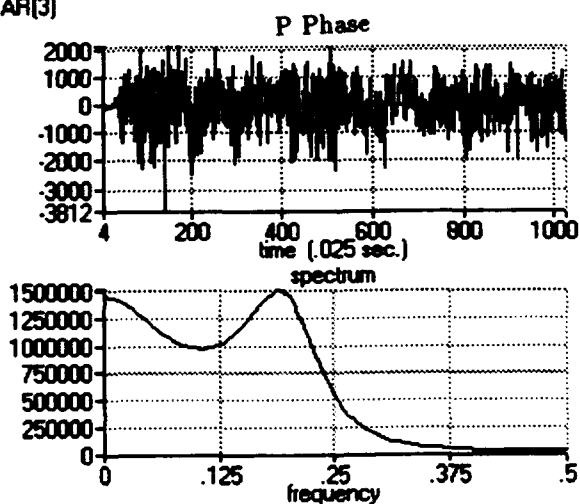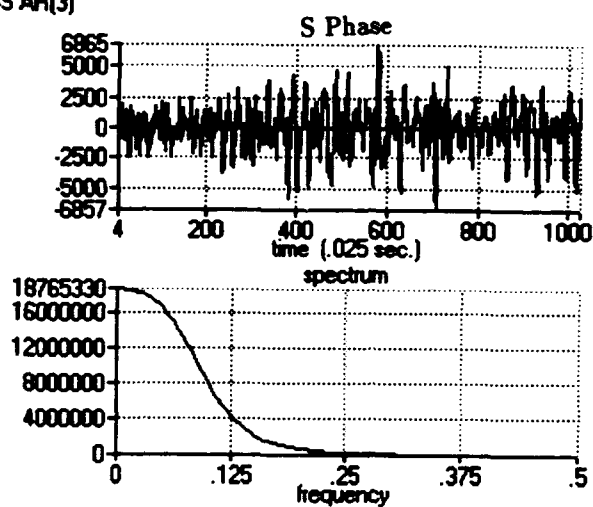
Figure A4: Earthquake 4 at Station F1A1 on 1/04/92 with local magnitude 3.60. P and S phases extracted are shown along with third-order autoregressive spectral estimators. The folding frequency is 20 Hz.
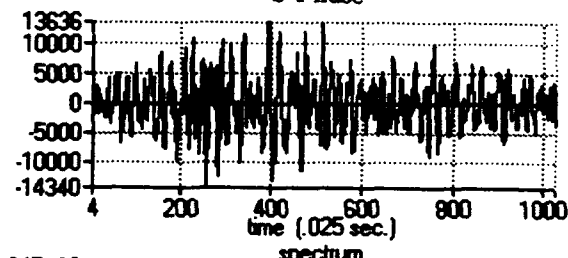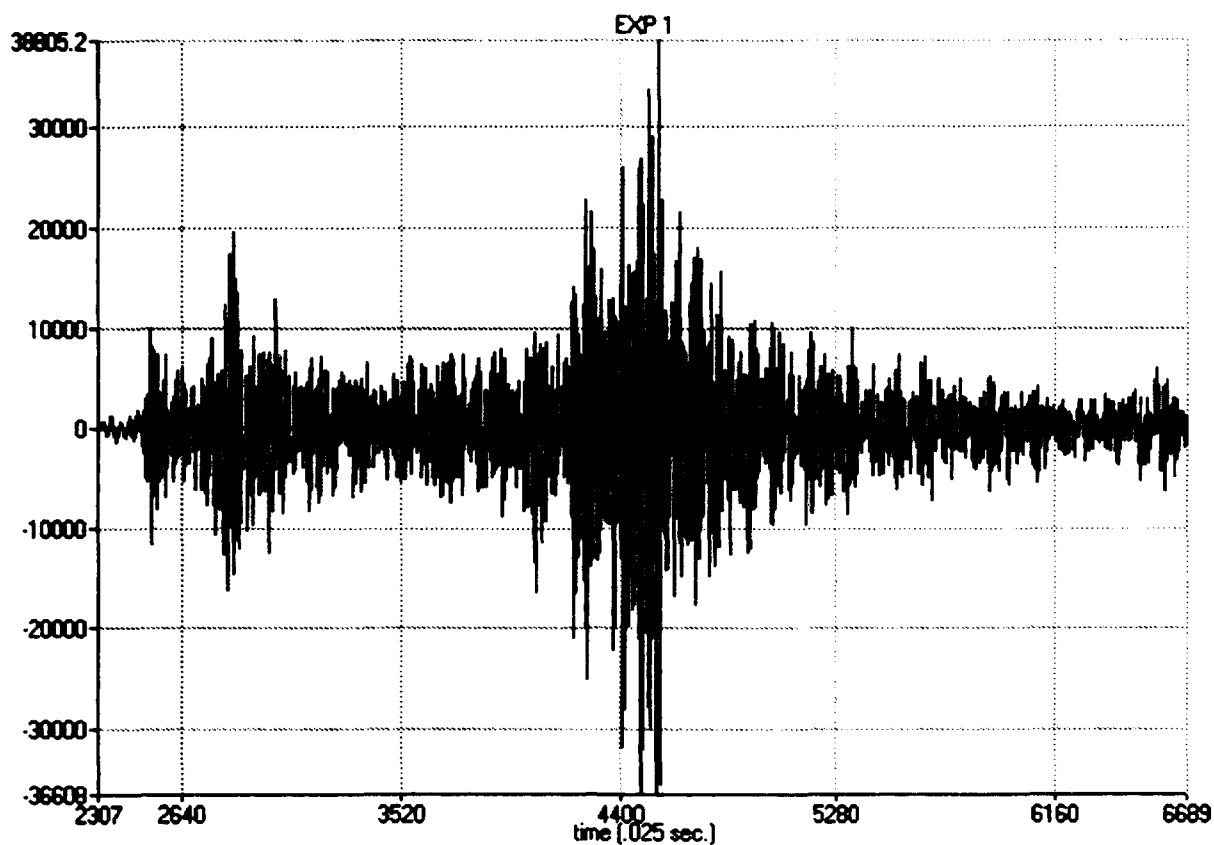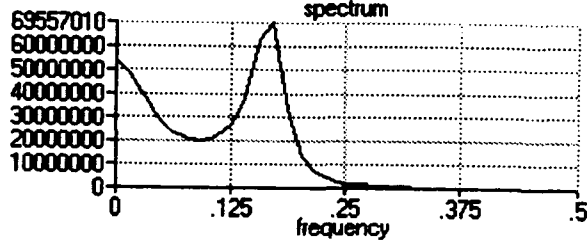
30
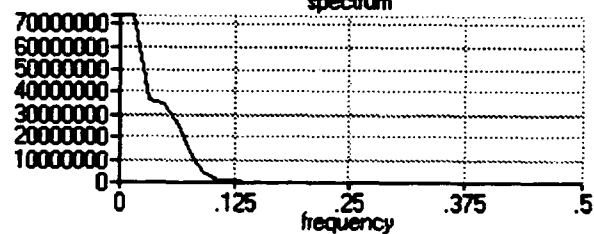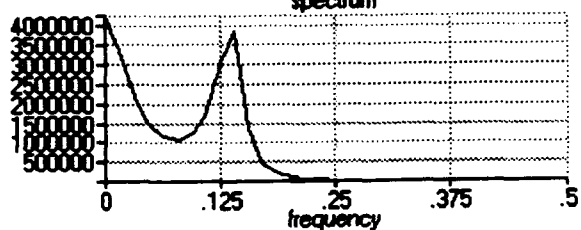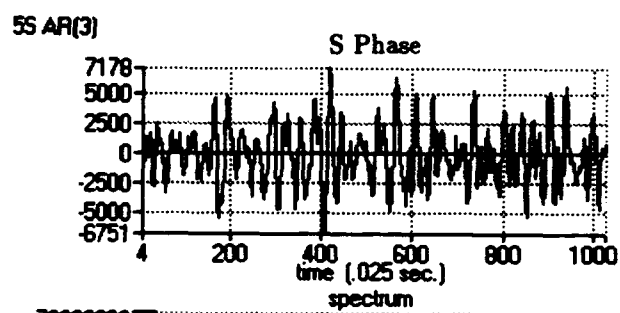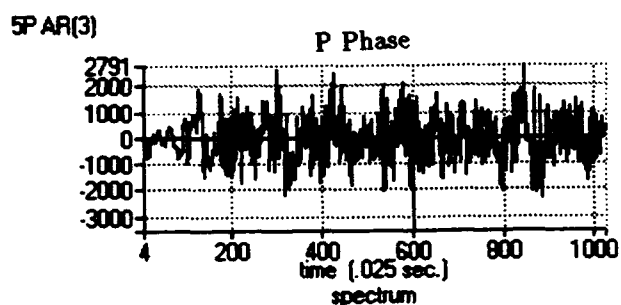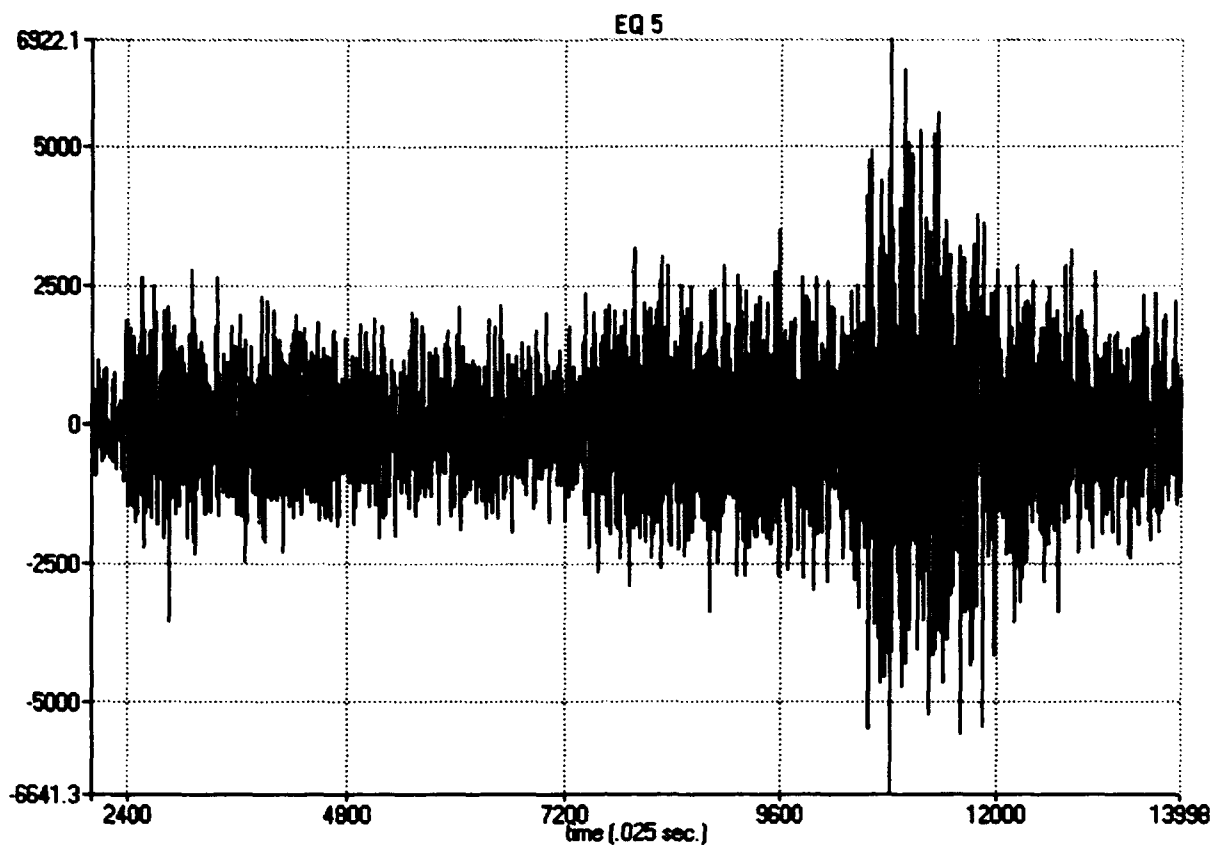
Figure A5: Earthquake 5 at Station ARA0 on 2/19/92 with local magnitude 3.26. P and S phases extracted are shown along with third-order autoregressive spectral estimators. The folding frequency is 20 Hz.
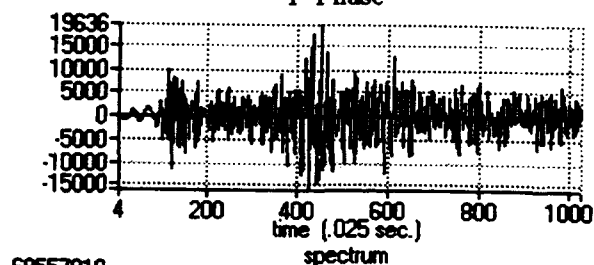
31
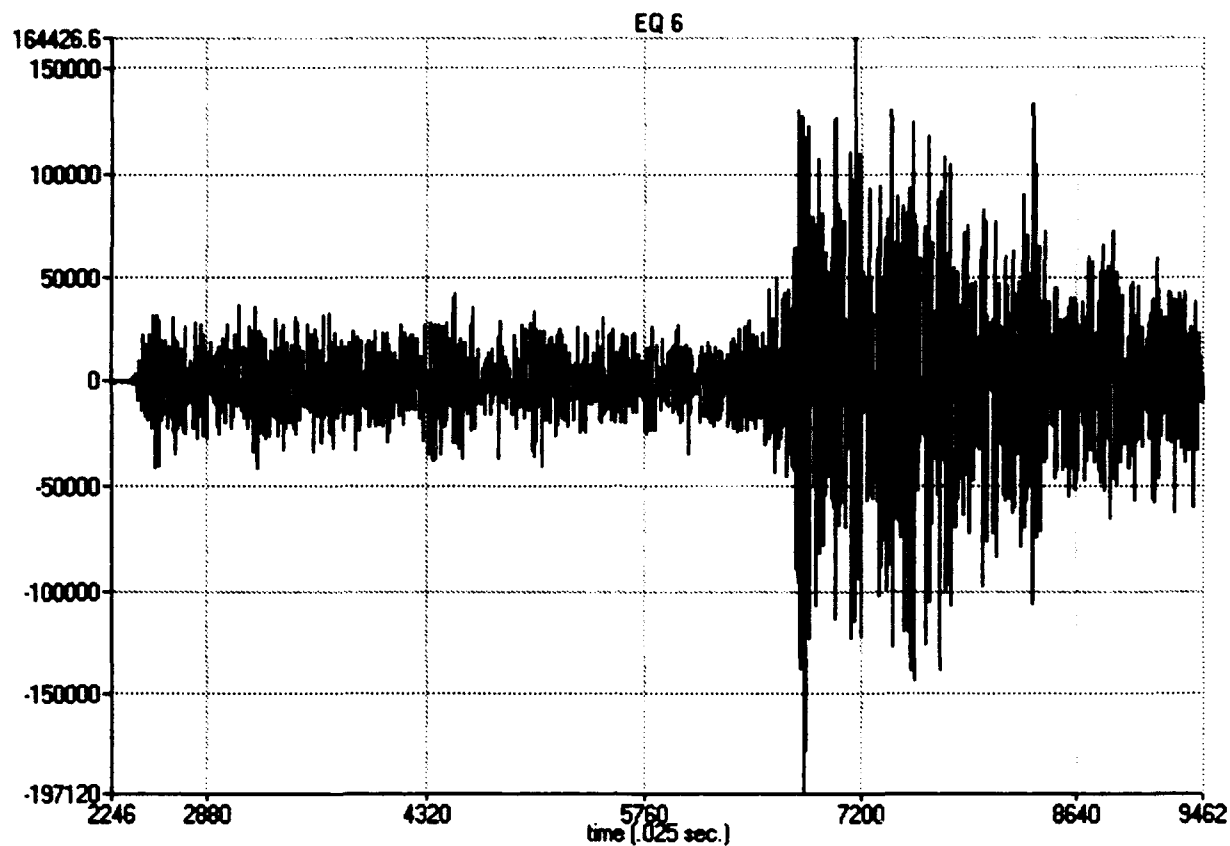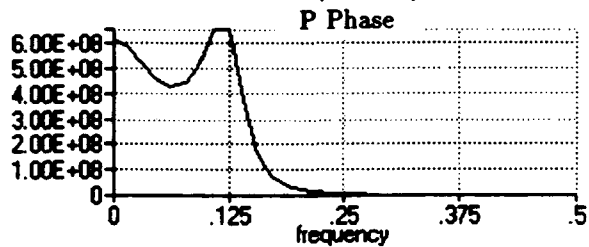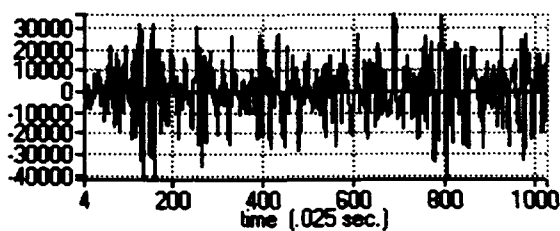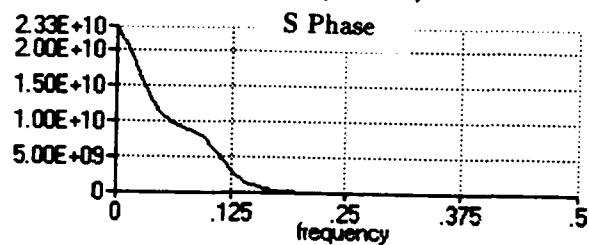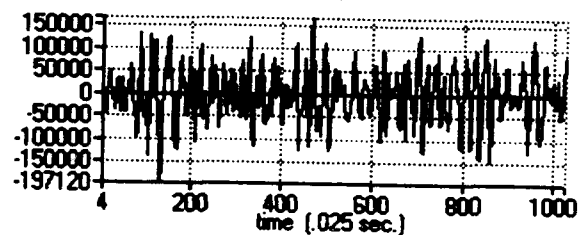
Figure A6: Earthquake 6 at Station NRA0 on 4/13/92 with local magnitude 4.40. P and S phases extracted are shown along with third-order autoregressive spectral estimators. The folding frequency is 20 Hz.

32
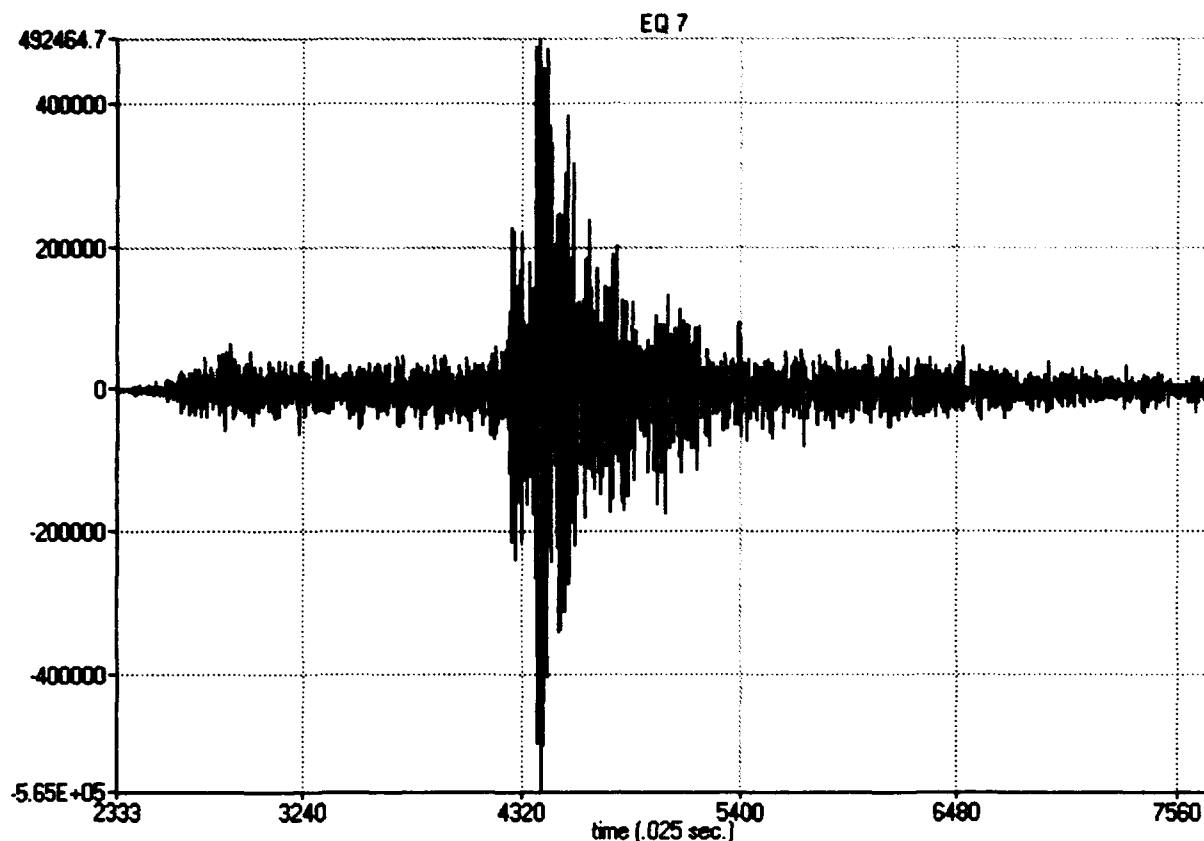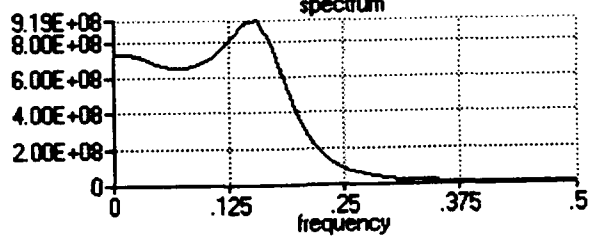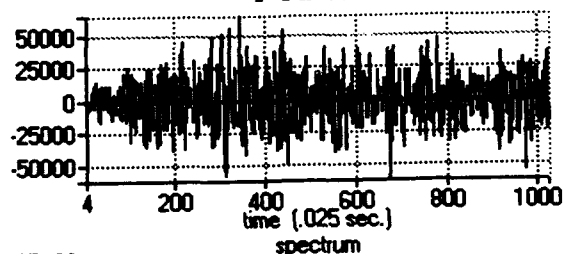
Figure A7: Earthquake 7 at Station NRA0 on 4/14/92 with local magnitude 3.38. P and S phases extracted are shown along with third-order autoregressive spectral estimators. The folding frequency is 20 Hz.

33

Figure A8: Earthquake 8 at Station NRA0 on 5/18/92 with local magnitude 2.74. P and S phases extracted are shown along with third-order autoregressive spectral estimators. The folding frequency is 20 Hz.
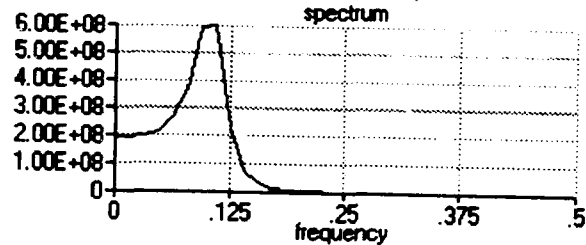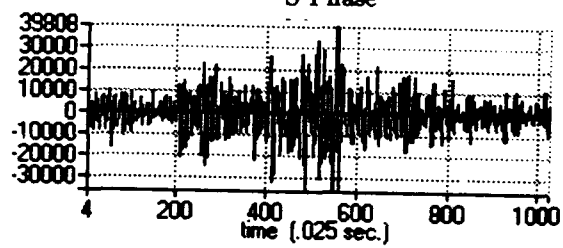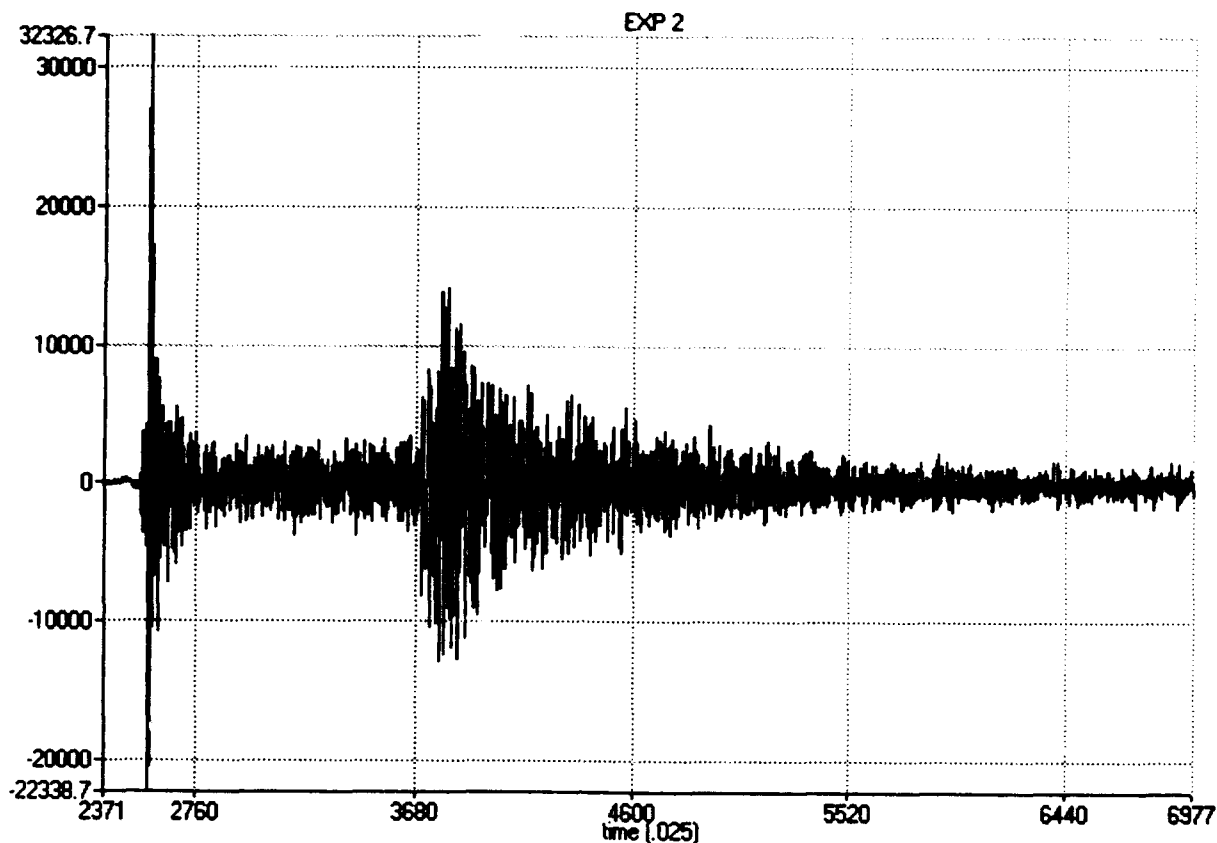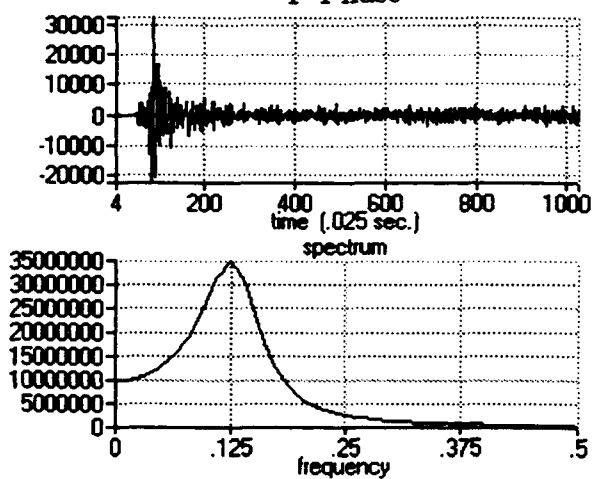
34

Figure A9: Explosion 1 at Station ARA0 on 3/23/91 with local magnitude 2.85. P and S phases extracted are shown along with third-order autoregressive spectral estimators. The folding frequency is 20 Hz.
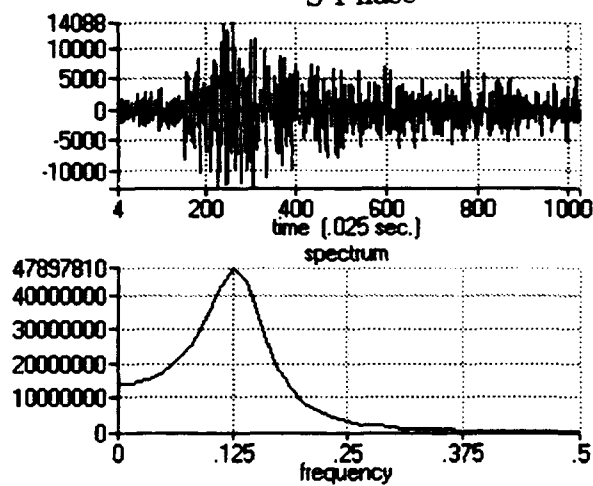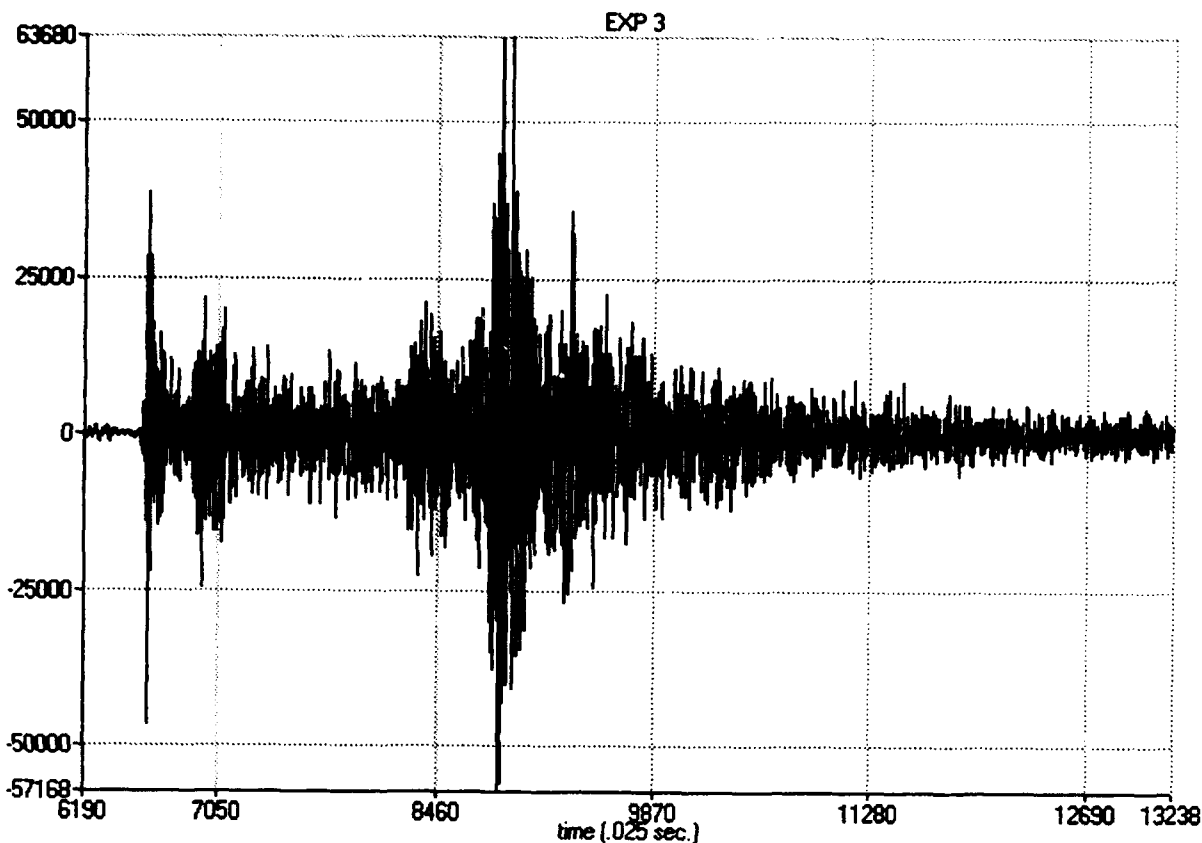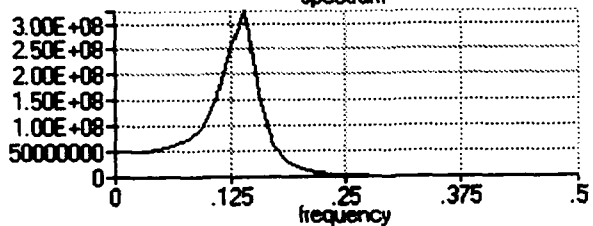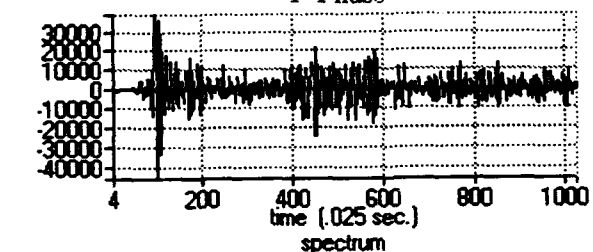
35

Figure A10: Explosion 2 at Station F1A1 on 4/13/91 with local magnitude 2.60. P and S phases extracted are shown along with third-order autoregressive spectral estimators. The folding frequency is 20 Hz.

36

Figure A11: Explosion 3 at Station ARA0 on 4/26/91 with local magnitude 2.95. P and S phases extracted are shown along with third-order autoregressive spectral estimators. The folding frequency is 20 Hz.
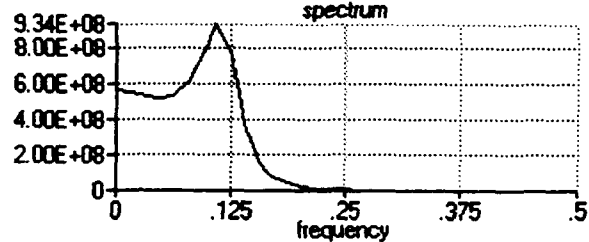
37

EXP 4

P Phase

S Phase
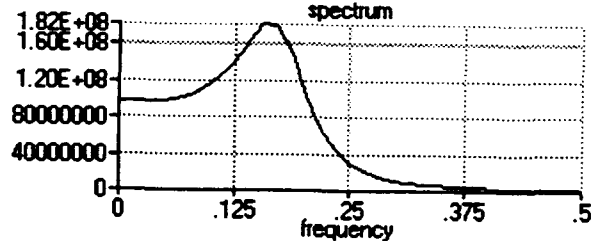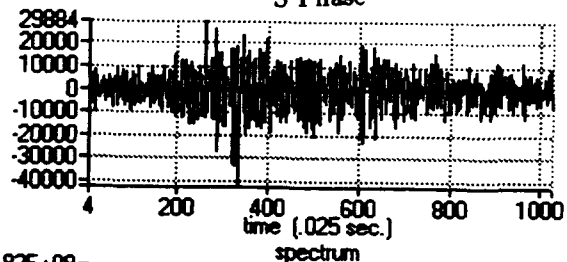
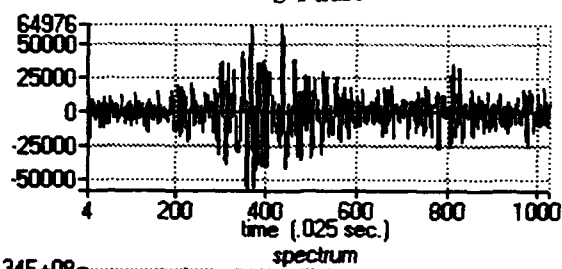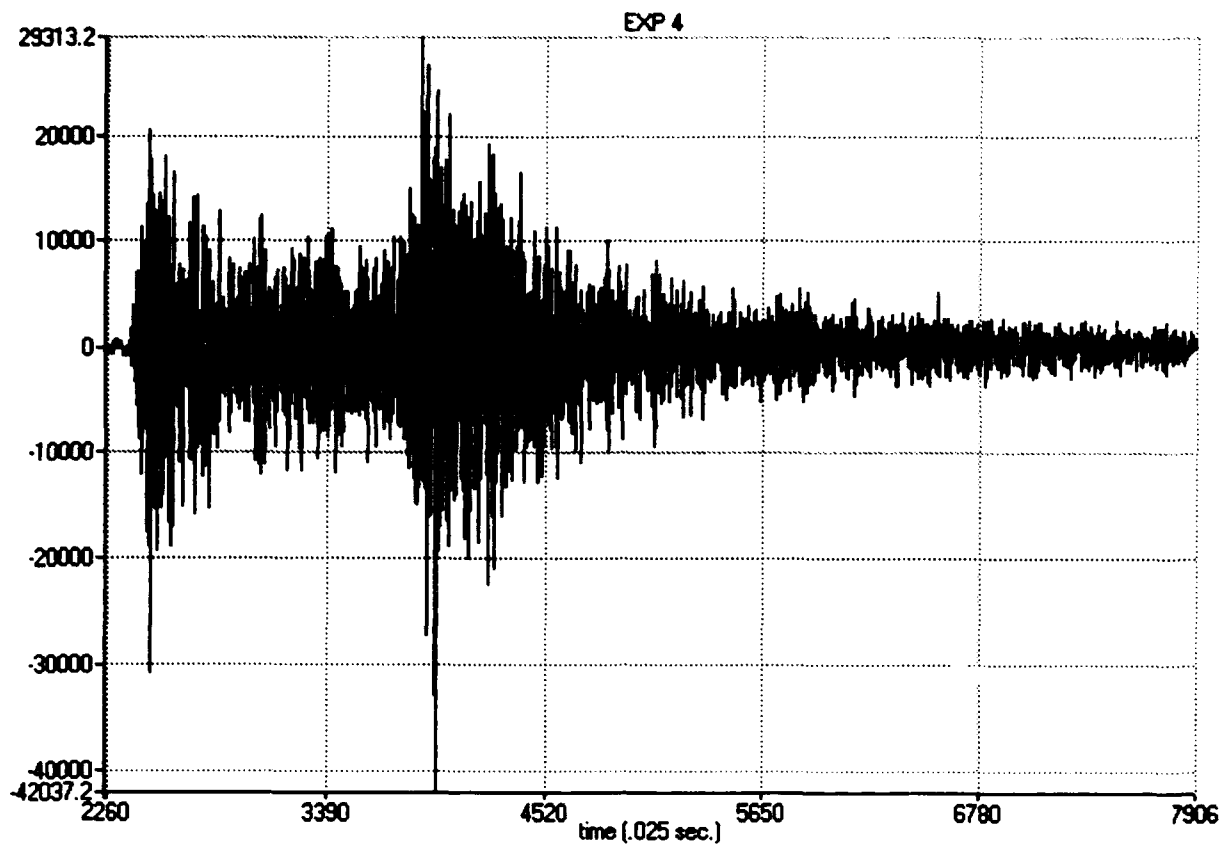spectrum

spectrum

Figure A12: Explosion 4 at Station ARA0 on 8/03/91 with local magnitude 2.13. P and S phases extracted are shown along with third-order autoregressive spectral estimators. The folding frequency is 20 Hz.

38
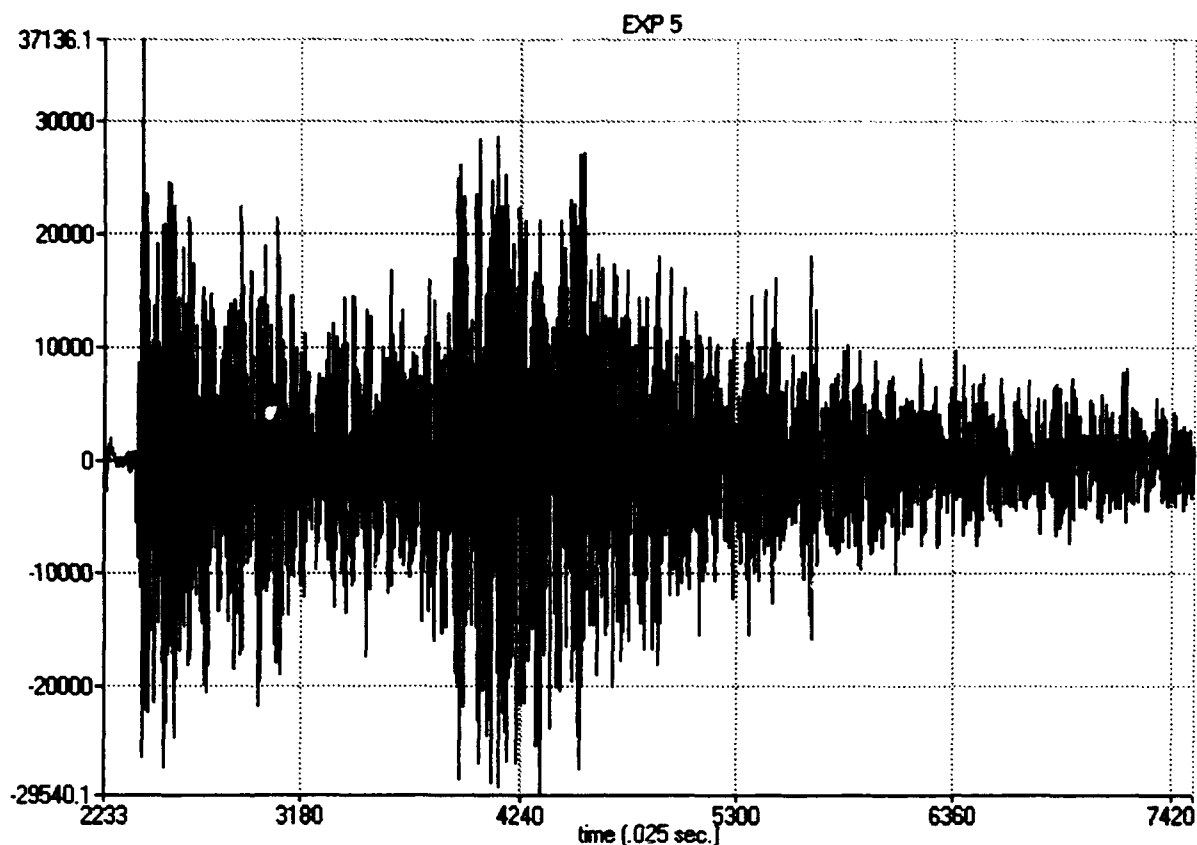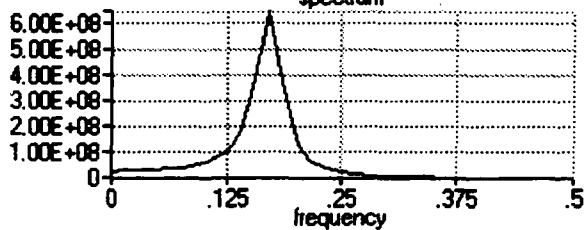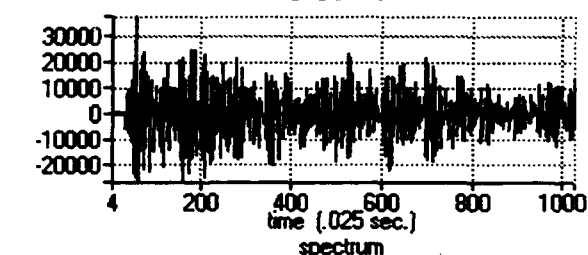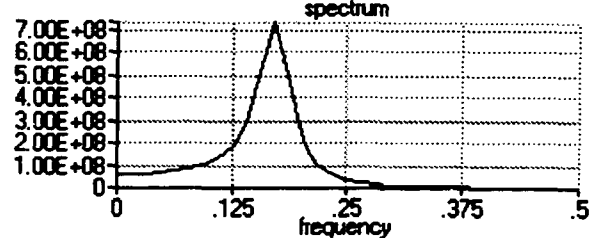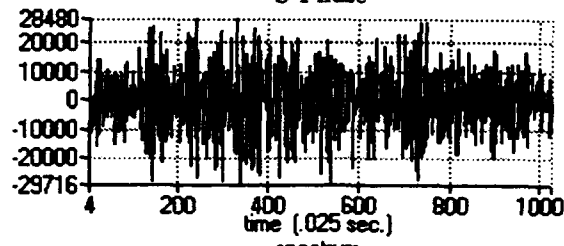
Figure A13: Explosion 5 at Station ARA0 on 9/05/91 with local magnitude 2.32. P and S phases extracted are shown along with third-order autoregressive spectral estimators. The folding frequency is 20 Hz.

39
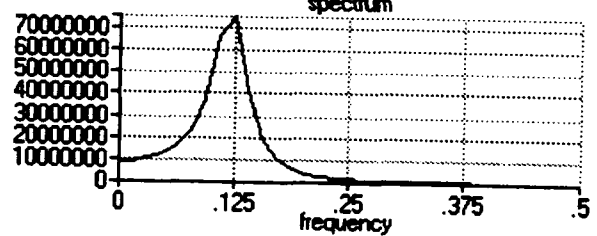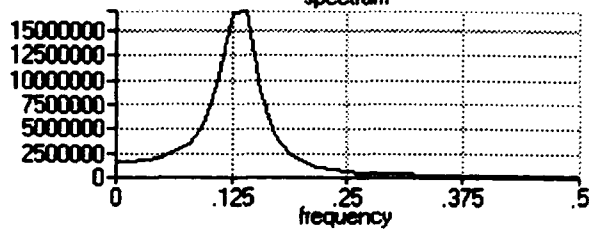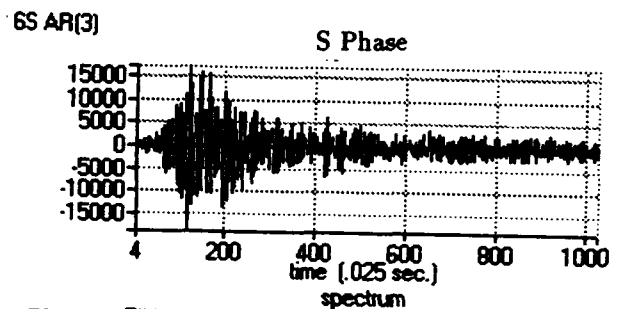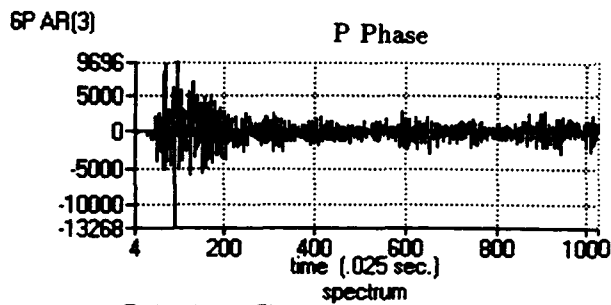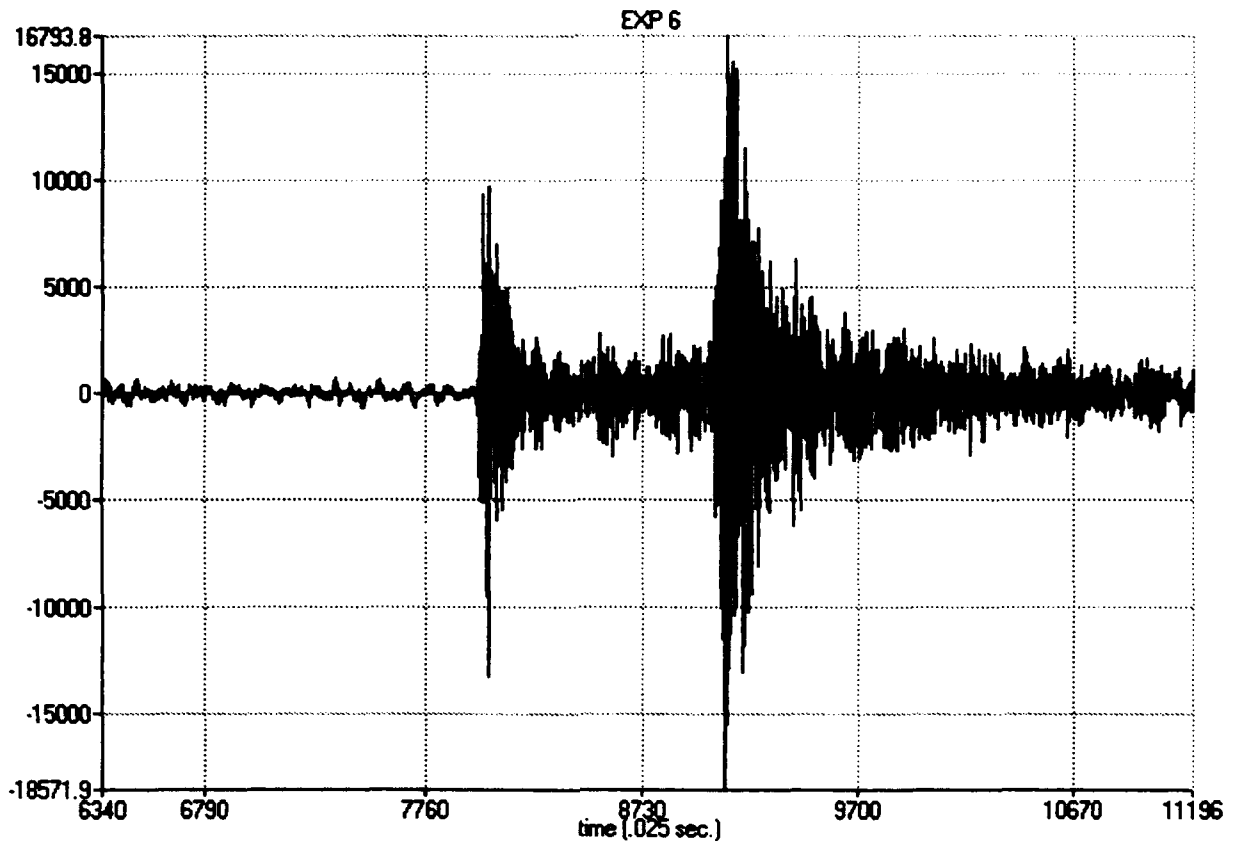
Figure A14: Explosion 6 at Station F1A1 on 12/10/91 with local magnitude 2.59. P and S phases extracted are shown along with third-order autoregressive spectral estimators. The folding frequency is 20 Hz.
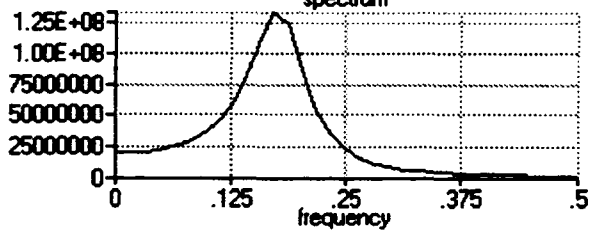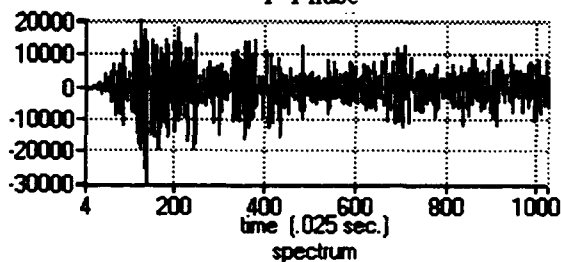
40
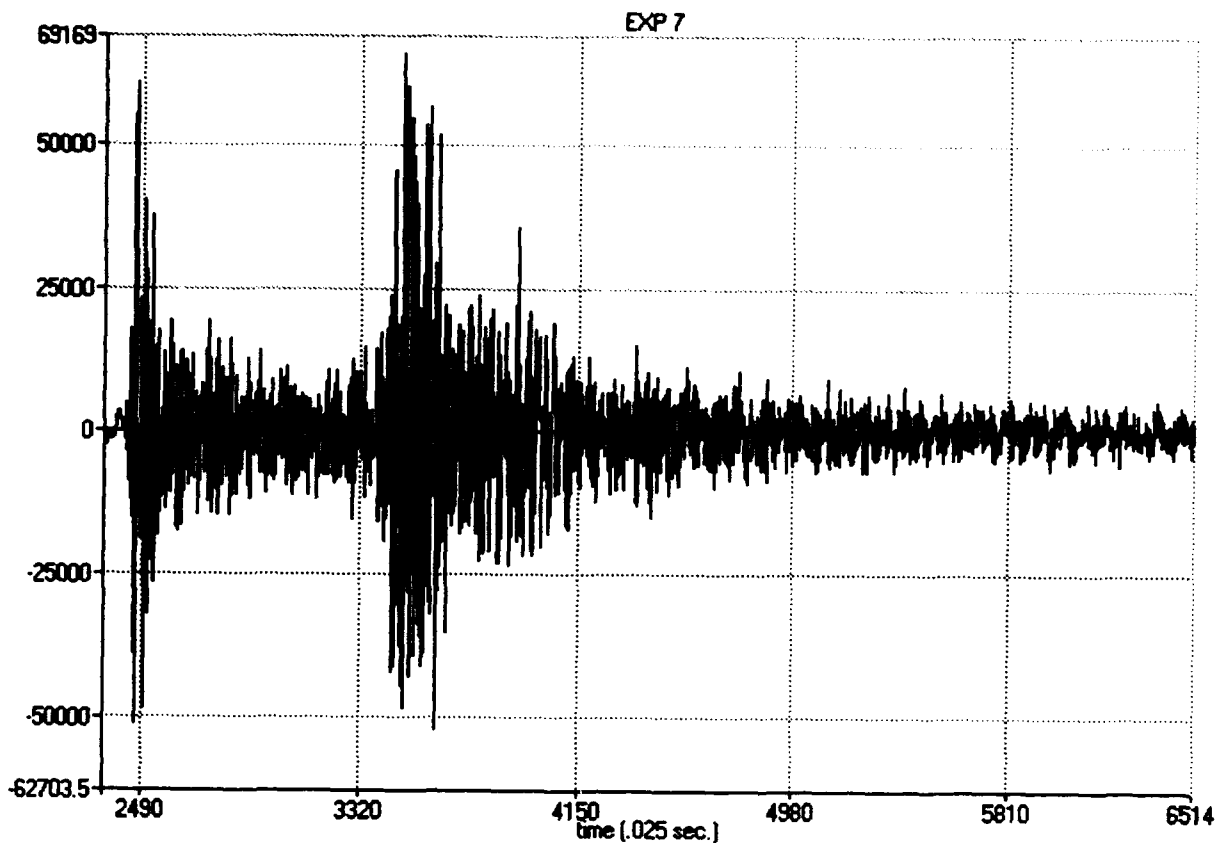
Figure A15: Explosion 7 at Station ARA0 on 12/29/91 with local magnitude 2.96. P and S phases extracted are shown along with third-order autoregressive spectral estimators. The folding frequency is 20 Hz.

41
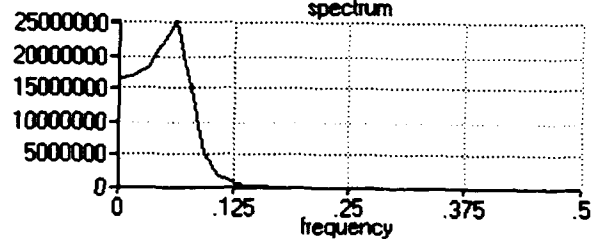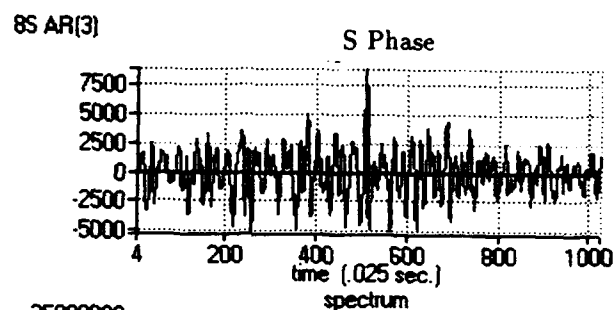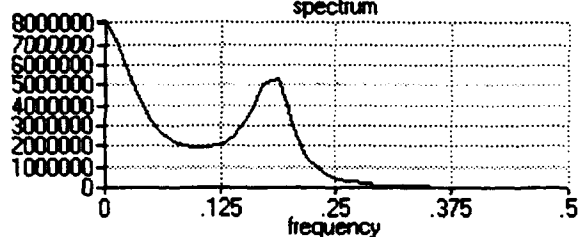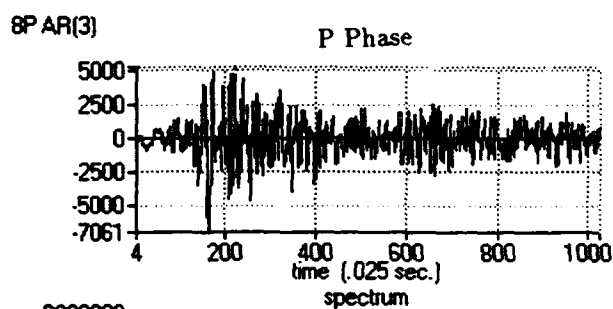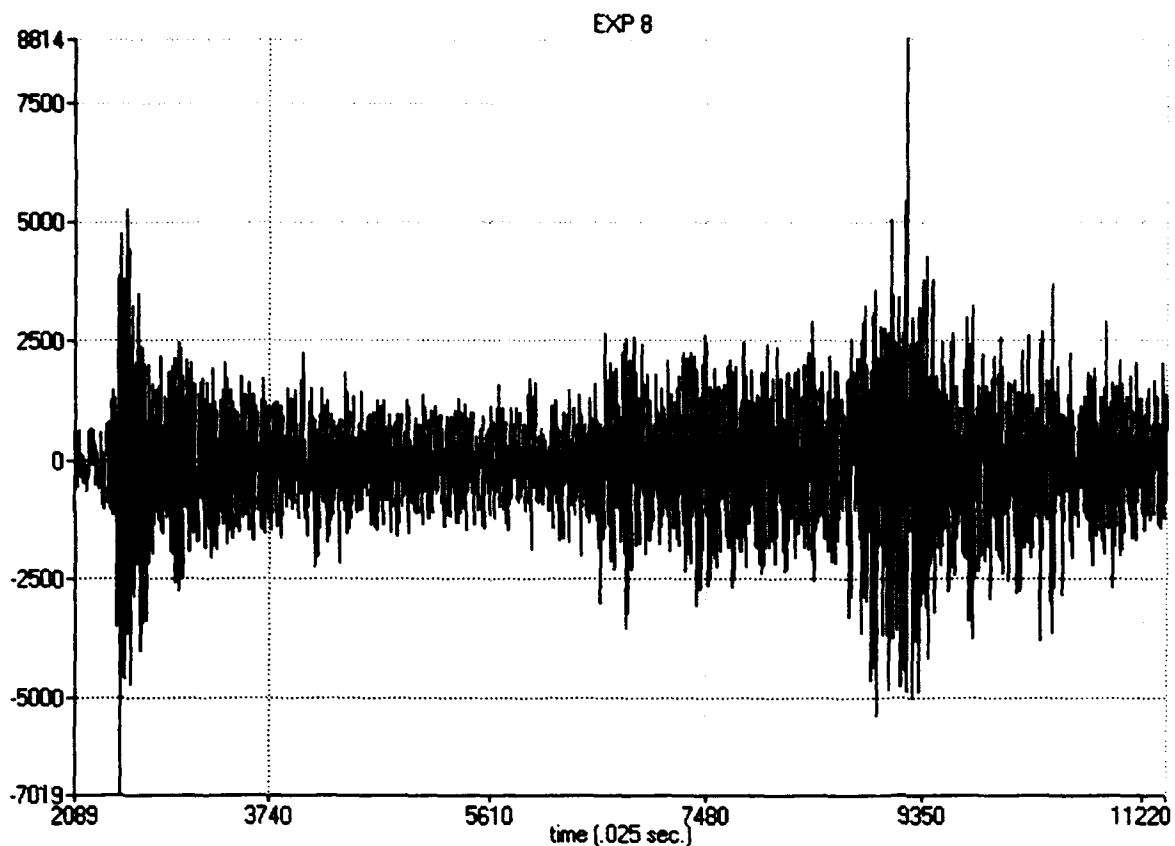
Figure A16: Explosion 8 at Station NRA0 on 3/25/92 with local magnitude 2.94. P and S phases extracted are shown along with third-order autoregressive spectral estimators. The folding frequency is 20 Hz (.5 cycles per point).

42

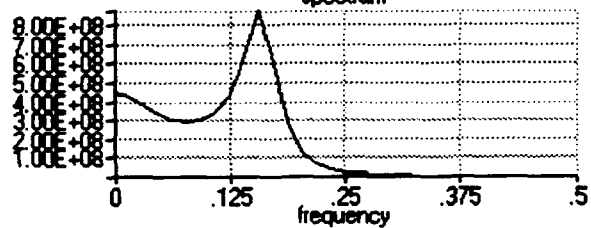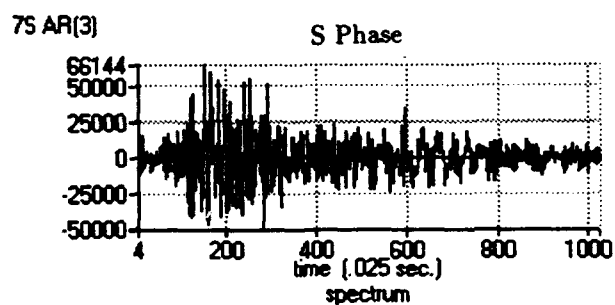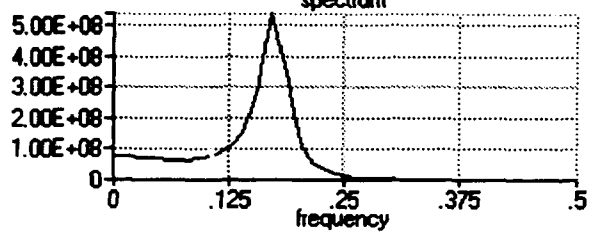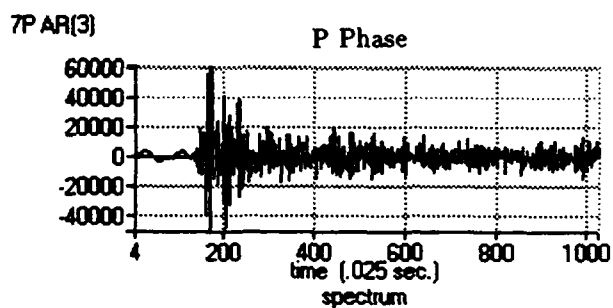Prof. Thomas Ahrens
Seismological Lab, 252-21
Division of Geological & Planetary Sciences
California Institute of Technology
Pasadena, CA 91125

Prof. Keiiti Aki
Center for Earth Sciences
University of Southern California
University Park
Los Angeles, CA 90089-0741

Prof. Shelton Alexander
Geosciences Department
403 Deike Building
The Pennsylvania State University
University Park, PA 16802

Prof. Charles B. Archambeau
CIRES
University of Colorado
Boulder, CO 80309

Dr. Thomas C. Bache, Jr.
Science Applications Int'l Corp.
10260 Campus Point Drive
San Diego, CA 92121 (2 copies)

Prof. Muawia Barazangi
Institute for the Study of the Continent
Cornell University
Ithaca, NY 14853

Dr. Jeff Barker
Department of Geological Sciences
State University of New York
 at Binghamton
Vestal, NY 13901

Dr. Douglas R. Baumgardt
ENSCO, Inc
5400 Port Royal Road
Springfield, VA 22151-2388

Dr. Susan Beck
Department of Geosciences
Building #77
University of Arizona
Tuscon, AZ 85721

Dr. T.J. Bennett
S-CUBED
A Division of Maxwell Laboratories
11800 Sunrise Valley Drive, Suite 1212
Reston, VA 22091

Dr. Robert Blandford
AFTAC/TT, Center for Seismic Studies
1300 North 17th Street
Suite 1450
Arlington, VA 22209-2308

Dr. Stephen Bratt
ARPA/NMRO
3701 North Fairfax Drive
Arlington, VA 22203-1714

Dr. Lawrence Burdick
IGPP, A-025
Scripps Institute of Oceanography
University of California, San Diego
La Jolla, CA 92093

Dr. Robert Burridge
Schlumberger-Doll Research Center
Old Quarry Road
Ridgefield, CT 06877

Dr. Jerry Carter
Center for Seismic Studies
1300 North 17th Street
Suite 1450
Arlington, VA 22209-2308

Dr. Eric Chael
Division 9241
Sandia Laboratory
Albuquerque, NM 87185

Dr. Martin Chapman
Department of Geological Sciences
Virginia Polytechnical Institute
21044 Derring Hall
Blacksburg, VA 24061

Prof. Vernon F. Cormier
Department of Geology & Geophysics
U-45, Room 207
University of Connecticut
Storrs, CT 06268

Prof. Steven Day
Department of Geological Sciences
San Diego State University
San Diego, CA 92182

Marvin Denny
U.S. Department of Energy
Office of Arms Control
Washington, DC 20585

1

Dr. Zoltan Der
ENSCO, Inc.
5400 Port Royal Road
Springfield, VA 22151-2388

Prof. Adam Dziewonski
Hoffman Laboratory, Harvard University
Dept. of Earth Atmos. & Planetary Sciences
20 Oxford Street
Cambridge, MA 02138

Prof. John Ebel
Department of Geology & Geophysics
Boston College
Chestnut Hill, MA 02167

Eric Fielding
SNEE Hall
INSTOC
Cornell University
Ithaca, NY 14853

Dr. Mark D. Fisk
Mission Research Corporation
735 State Street
P.O. Drawer 719
Santa Barbara, CA 93102

Prof Stanley Flatte
Applied Sciences Building
University of California, Santa Cruz
Santa Cruz, CA 95064

Dr. John Foley
NER-Geo Sciences
1100 Crown Colony Drive
Quincy, MA 02169

Prof. Donald Forsyth
Department of Geological Sciences
Brown University
Providence, RI 02912

Dr. Art Frankel
U.S. Geological Survey
922 National Center
Reston, VA 22092

Dr. Cliff Frolich
Institute of Geophysics
8701 North Mopac
Austin, TX 78759

Dr. Holly Given
IGPP, A-025
Scripps Institute of Oceanography
University of California, San Diego
La Jolla, CA 92093

Dr. Jeffrey W. Given
SAIC
10260 Campus Point Drive
San Diego, CA 92121

Dr. Dale Glover
Defense Intelligence Agency
ATTN: ODT-1B
Washington, DC 20301

Dan N. Hagedon
Pacific Northwest Laboratories
Battelle Boulevard
Richland, WA 99352

Dr. James Hannon
Lawrence Livermore National Laboratory
P.O. Box 808
L-205
Livermore, CA 94550

Prof. David G. Harkrider
Seismological Laboratory
Division of Geological & Planetary Sciences
California Institute of Technology
Pasadena, CA 91125

Prof. Danny Harvey
CIRES
University of Colorado
Boulder, CO 80309

Prof. Donald V. Helmberger
Seismological Laboratory
Division of Geological & Planetary Sciences
California Institute of Technology
Pasadena, CA 91125

Prof. Eugene Herrin
Institute for the Study of Earth and Man
Geophysical Laboratory
Southern Methodist University
Dallas, TX 75275

Prof. Robert B. Herrmann
Department of Earth & Atmospheric Sciences
St. Louis University
St. Louis, MO 63156

Prof. Lane R. Johnson
Seismographic Station
University of California
Berkeley, CA 94720

Prof. Thomas H. Jordan
Department of Earth, Atmospheric &
 Planetary Sciences
Massachusetts Institute of Technology
Cambridge, MA 02139

Prof. Alan Kafka
Department of Geology & Geophysics
Boston College
Chestnut Hill, MA 02167

Robert C. Kemerait
ENSCO, Inc.
445 Pineda Court
Melbourne, FL 32940

Dr. Karl Koch
Institute for the Study of Earth and Man
Geophysical Laboratory
Southern Methodist University
Dallas, Tx 75275

Dr. Max Koontz
U.S. Dept. of Energy/DP 5
Forrestal Building
1000 Independence Avenue
Washington, DC 20585

Dr. Richard LaCoss
MIT Lincoln Laboratory, M-200B
P.O. Box 73
Lexington, MA 02173-0073

Dr. Fred K. Lamb
University of Illinois at Urbana-Champaign
Department of Physics
1110 West Green Street
Urbana, IL 61801

Prof. Charles A. Langston
Geosciences Department
403 Deike Building
The Pennsylvania State University
University Park, PA 16802

Jim Lawson, Chief Geophysicist
Oklahoma Geological Survey
Oklahoma Geophysical Observatory
P.O. Box 8
Leonard, OK 74043-0008

Prof. Thorne Lay
Institute of Tectonics
Earth Science Board
University of California, Santa Cruz
Santa Cruz, CA 95064

Dr. William Leith
U.S. Geological Survey
Mail Stop 928
Reston, VA 22092

Mr. James F. Lewkowicz
Phillips Laboratory/GPEH
29 Randolph Road
Hanscom AFB, MA 01731-3010(2 copies)

Mr. Alfred Lieberman
ACDA/VI-OA State Department Building
Room 5726
320-21st Street, NW
Washington, DC 20451

Prof. L. Timothy Long
School of Geophysical Sciences
Georgia Institute of Technology
Atlanta, GA 30332

Dr. Randolph Martin, III
New England Research, Inc.
76 Olcott Drive
White River Junction, VT 05001

Dr. Robert Masse
Denver Federal Building
Box 25046, Mail Stop 967
Denver, CO 80225

Dr. Gary McCartor
Department of Physics
Southern Methodist University
Dallas, TX 75275

Prof. Thomas V. McEvilly
Seismographic Station
University of California
Berkeley, CA 94720

Dr. Art McGarr
U.S. Geological Survey
Mail Stop 977
U.S. Geological Survey
Menlo Park, CA 94025

Dr. Keith L. McLaughlin
S-CUBED
A Division of Maxwell Laboratory
P.O. Box 1620
La Jolla, CA 92038-1620

Dr. Jay J. Pulli
Radix Systems, Inc.
201 Perry Parkway
Gaithersburg, MD 20877

Stephen Miller & Dr. Alexander Florence
SRI International
333 Ravenswood Avenue
Box AF 116
Menlo Park, CA 94025-3493

Dr. Robert Reinke
ATTN: FCTVTD
Field Command
Defense Nuclear Agency
Kirtland AFB, NM 87115

Prof. Bernard Minster
IGPP, A-025
Scripps Institute of Oceanography
University of California, San Diego
La Jolla, CA 92093

Prof. Paul G. Richards
Lamont-Doherty Geological Observatory
 of Columbia University
Palisades, NY 10964

Prof. Brian J. Mitchell
Department of Earth & Atmospheric Sciences
St. Louis University
St. Louis, MO 63156

Mr. Wilmer Rivers
Teledyne Geotech
314 Montgomery Street
Alexandria, VA 22314

Mr. Jack Murphy
S-CUBED
A Division of Maxwell Laboratory
11800 Sunrise Valley Drive, Suite 1212
Reston, VA 22091 (2 Copies)

Dr. Alan S. Ryall, Jr.
ARPA/NMRO
3701 North Fairfax Drive
Arlington, VA 22209-1714

Dr. Keith K. Nakanishi
Lawrence Livermore National Laboratory
L-025
P.O. Box 808
Livermore, CA 94550

Dr. Richard Sailor
TASC, Inc.
55 Walkers Brook Drive
Reading, MA 01867

Prof. John A. Orcutt
IGPP, A-025
Scripps Institute of Oceanography
University of California, San Diego
La Jolla, CA 92093

Prof. Charles G. Sammis
Center for Earth Sciences
University of Southern California
University Park
Los Angeles, CA 90089-0741

Prof. Jeffrey Park
Kline Geology Laboratory
P.O. Box 6666
New Haven, CT 06511-8130

Prof. Christopher H. Scholz
Lamont-Doherty Geological Observatory
 of Columbia University
Palisades, NY 10964

Dr. Howard Patton
Lawrence Livermore National Laboratory
L-025
P.O. Box 808
Livermore, CA 94550

Dr. Susan Schwartz
Institute of Tectonics
1156 High Street
Santa Cruz, CA 95064

Dr. Frank Pilotte
HQ AFTAC/TT
130 South Highway A1A
Patrick AFB, FL 32925-3002

Secretary of the Air Force
(SAFRD)
Washington, DC 20330

4

Office of the Secretary of Defense
DDR&E
Washington, DC 20330

Thomas J. Sereno, Jr.
Science Application Int'l Corp.
10260 Campus Point Drive
San Diego, CA 92121

Dr. Michael Shore
Defense Nuclear Agency/SPSS
6801 Telegraph Road
Alexandria, VA 22310

Dr. Robert Shumway
University of California Davis
Division of Statistics
Davis, CA 95616

Dr. Matthew Sibol
Virginia Tech
Seismological Observatory
4044 Derring Hall
Blacksburg, VA 24061-0420

Prof. David G. Simpson
IRIS, Inc.
1616 North Fort Myer Drive
Suite 1050
Arlington, VA 22209

Donald L. Springer
Lawrence Livermore National Laboratory
L-025
P.O. Box 808
Livermore, CA 94550

Dr. Jeffrey Stevens
S-CUBED
A Division of Maxwell Laboratory
P.O. Box 1620
La Jolla, CA 92038-1620

Lt. Col. Jim Stobie
ATTN: AFOSR/NL
110 Duncan Avenue
Bolling AFB
Washington, DC 20332-0001

Prof. Brian Stump
Institute for the Study of Earth & Man
Geophysical Laboratory
Southern Methodist University
Dallas, TX 75275

Prof. Jeremiah Sullivan
University of Illinois at Urbana-Champaign
Department of Physics
1110 West Green Street
Urbana, IL 61801

Prof. L. Sykes
Lamont-Doherty Geological Observatory
 of Columbia University
Palisades, NY 10964

Dr. David Taylor
ENSCO, Inc.
445 Pineda Court
Melbourne, FL 32940

Dr. Steven R. Taylor
Los Alamos National Laboratory
P.O. Box 1663
Mail Stop C335
Los Alamos, NM 87545

Prof. Clifford Thurber
University of Wisconsin-Madison
Department of Geology & Geophysics
1215 West Dayton Street
Madison, WS 53706

Prof. M. Nafi Toksoz
Earth Resources Lab
Massachusetts Institute of Technology
42 Carleton Street
Cambridge, MA 02142

Dr. Larry Turnbull
CIA-OSWR/NED
Washington, DC 20505

Dr. Gregory van der Vink
IRIS, Inc.
1616 North Fort Myer Drive
Suite 1050
Arlington, VA 22209

Dr. Karl Veith
EG&G
5211 Auth Road
Suite 240
Suitland, MD 20746

Prof. Terry C. Wallace
Department of Geosciences
Building #77
University of Arizona
Tuscon, AZ 85721

Dr. Thomas Weaver
Los Alamos National Laboratory
P.O. Box 1663
Mail Stop C335
Los Alamos, NM 87545

Dr. William Wortman
Mission Research Corporation
8560 Cinderbed Road
Suite 700
Newington, VA 22122

Prof. Francis T. Wu
Department of Geological Sciences
State University of New York
 at Binghamton
Vestal, NY 13901

ARPA, OASB/Library
3701 North Fairfax Drive
Arlington, VA 22203-1714

HQ DNA
ATTN: Technical Library
Washington, DC 20305

Defense Intelligence Agency
Directorate for Scientific & Technical Intelligence
ATTN: DTIB
Washington, DC 20340-6158

Defense Technical Information Center
Cameron Station
Alexandria, VA 22314 (2 Copies)

TACTEC
Battelle Memorial Institute
505 King Avenue
Columbus, OH 43201 (Final Report)

Phillips Laboratory
ATTN: XPG
29 Randolph Road
Hanscom AFB, MA 01731-3010

Phillips Laboratory
ATTN: GPE
29 Randolph Road
Hanscom AFB, MA 01731-3010

Phillips Laboratory
ATTN: TSML
5 Wright Street
Hanscom AFB, MA 01731-3004

Phillips Laboratory
ATTN: PL/SUL
3550 Aberdeen Ave SE
Kirtland, NM 87117-5776 (2 copies)

Dr. Michel Bouchon
I.R.I.G.M.-B.P. 68
38402 St. Martin D'Heres
Cedex, FRANCE

Dr. Michel Campillo
Observatoire de Grenoble
I.R.I.G.M.-B.P. 53
38041 Grenoble, FRANCE

Dr. Kin Yip Chun
Geophysics Division
Physics Department
University of Toronto
Ontario, CANADA

Prof. Hans-Peter Harjes
Institute for Geophysic
Ruhr University/Bochum
P.O. Box 102148
4630 Bochum 1, GERMANY

Prof. Eystein Husebye
NTNF/NORSAR
P.O. Box 51
N-2007 Kjeller, NORWAY

David Jepsen
Acting Head, Nuclear Monitoring Section
Bureau of Mineral Resources
Geology and Geophysics
G.P.O. Box 378, Canberra, AUSTRALIA

Ms. Eva Johannisson
Senior Research Officer
FOA
S-172 90 Sundbyberg, SWEDEN

Dr. Peter Marshall
Procurement Executive
Ministry of Defense
Blacknest, Brimpton
Reading FG7-FRS, UNITED KINGDOM

6

Dr. Bernard Massinon, Dr. Pierre Mechler
Societe Radiomana
27 rue Claude Bernard
75005 Paris, FRANCE (2 Copies)

Dr. Svein Mykkeltveit
NTNT/NORSAR
P.O. Box 51
N-2007 Kjeller, NORWAY (3 Copies)

Prof. Keith Priestley
University of Cambridge
Bullard Labs, Dept. of Earth Sciences
Madingley Rise, Madingley Road
Cambridge CB3 OEZ, ENGLAND

Dr. Jorg Schlittenhardt
Federal Institute for Geosciences & Nat'l Res.
Postfach 510153
D-30631 Hannover , GERMANY

Dr. Johannes Schweitzer
Institute of Geophysics
Ruhr University/Bochum
P.O. Box 1102148
4360 Bochum 1, GERMANY

Trust & Verify
VERTIC
8 John Adam Street
London WC2N 6EZ, ENGLAND